J. exp. Biol. 158, 63–95 (1991)
Printed in Great Britain © The Company of Biologists Limited 1991

THE WHOLE-BODY WITHDRAWAL RESPONSE OF *LYMNAEA STAGNALIS*

I. IDENTIFICATION OF CENTRAL MOTONEURONES AND MUSCLES

BY GRAHAM P. FERGUSON* AND PAUL R. BENJAMIN

Sussex Invertebrate Neuroscience Group, School of Biology, University of Sussex, Brighton BN1 9QG, United Kingdom

Accepted 4 February 1991

Summary

Two muscle systems mediated the whole-body withdrawal response of *Lymnaea stagnalis*: the columellar muscle (CM) and the dorsal longitudinal muscle (DLM). The CM was innervated by the columellar nerves and contracted longitudinally to shorten the ventral head-foot complex and to pull the shell forward and down over the body. The DLM was innervated by the superior and inferior cervical nerves and the left and right parietal nerves. During whole-body withdrawal, the DLM contracted synchronously with the CM and shortened the dorsal head-foot longitudinally. The CM and the DLM were innervated by a network of motoneurones. The somata of these cells were located in seven ganglia of the central nervous system (CNS), but were especially concentrated in the bilaterally symmetrical A clusters of the cerebral ganglia. The CM was innervated by cells in the cerebral and pedal ganglia and the DLM by cells in the cerebral, pedal, pleural and left parietal ganglia. Individual motoneurones innervated large, but discrete, areas of muscle, which often overlapped with those innervated by other motoneurones. Motoneuronal action potentials evoked one-for-one non-facilitating excitatory junction potentials within muscle fibres. No all-or-nothing action potentials were recorded in the CM or DLM, and they did not appear to be innervated by inhibitory motoneurones. The whole network of motoneurones was electrotonically coupled, with most cells on one side of the CNS strongly coupled to each other but weakly coupled to cells on the contralateral side of the CNS. This electrotonic coupling between motoneurones is probably important in producing synchronous contraction of the CM and DLM when the animal retracts its head-foot complex during whole-body withdrawal.

Introduction

Withdrawal and escape responses are stereotyped, relatively simple patterns of behaviour in which an obvious motor output is evoked by a definite sensory input. These features make them good model systems for the cellular analysis of the

* Present address: Stazione Zoologica, Villa Comunale, I-80121 Napoli, Italy.

Key words: mollusc, pond snail, withdrawal behaviour, motor control, *Lymnaea stagnalis*.

neural circuitry producing the response. Consequently, withdrawal and escape responses of many different species, especially those mediated by giant fibre systems (reviewed by Bullock, 1984), have been used for neuroethological studies.

The two gastropod escape and withdrawal responses most thoroughly investigated neurophysiologically are *Tritonia diomedia* escape swimming (Willows, 1967; Willows *et al.* 1973; reviewed by Getting, 1983) and *Aplysia californica* gill and siphon withdrawal (Kupfermann and Kandel, 1969; reviewed by Kandel, 1976, 1979). In *Tritonia*, contact with a predatory starfish excites a network of premotor interneurones to produce two different motor programmes: a reflexive withdrawal away from the starfish, followed by rhythmic escape swimming (Getting and Dekin, 1985). In contrast, *Aplysia* gill and siphon withdrawal is a localised contraction that consists of the retraction of the gill and siphon into the mantle cavity and the closing together of the parapodia (Kupfermann and Kandel, 1969). This behaviour is elicited by tactile stimulation of the mantle and siphon area and consists of reflexive contractions mediated centrally (Kupfermann *et al.* 1974) and peripherally (Peretz *et al.* 1976) and all-or-nothing contractions mediated by activity in a central pattern generator (Kupfermann *et al.* 1974; Pinsker *et al.* 1970; Kanz *et al.* 1979).

The defensive whole-body withdrawal response of the freshwater pulmonate *Lymnaea stagnalis* (L.) is induced by photic (shadow) and tactile stimuli and differs from *Tritonia* escape swimming and *Aplysia* gill and siphon withdrawal because a whole-body withdrawal of the head-foot, into the shell, occurs and the animal then becomes stationary. The withdrawal behaviours induced by the two sensory modalities are slightly different. In response to a shadow passing over the animal a very stereotyped withdrawal occurs: the tentacles are flattened, the head-foot is shortened longitudinally and the shell is pulled forward and down to cover it (Cook, 1970). In contrast, the response to tactile stimuli is graded (depending on stimulus intensity), varies according to the part of the body stimulated and includes several components which occur in sequence as the intensity of the stimulus is increased (Lever *et al.* 1977). The major differences between the withdrawal responses to the different sensory modalities are that the tactile response begins as a local contraction away from the site of stimulation while the timing of the tentacle contractions varies when different parts of the body are stimulated (Lever *et al.* 1977). Also, the latency of the response to tactile stimuli is shorter than that to shadow stimuli (0.2 s *versus* 0.5 s; Ferguson, 1985). The major components of the whole-body withdrawal response to either sensory modality are the longitudinal shortening of the head-foot and the pulling of the shell forward to cover it. These are very similar irrespective of the modality of the sensory stimulus inducing withdrawal and are the components that have been investigated in this study.

Previous studies have examined the gross morphology of the musculature of *Lymnaea* and have demonstrated that the muscles used during whole-body withdrawal contain unstriated fibres similar to vertebrate smooth muscle (Plesch *et al.* 1975). In addition, lesion studies have identified some of the central and

peripheral pathways necessary for production of the response (Cook, 1975). However, these investigations gave no information about the central neuronal mechanisms underlying the whole-body withdrawal response. Considerably more work has been done on the peripheral pathways involved in carrying tactile and photic sensory input to the CNS and this is reviewed in the following paper (Ferguson and Benjamin, 1991).

In this paper, we describe the morphology and mode of action of the two muscle systems mediating the whole-body withdrawal response of *Lymnaea* and provide evidence that the muscles are innervated by a population of centrally located motoneurones. Unlike other molluscan motor systems where motoneurones are confined to one ganglion or to a pair of bilaterally symmetrical ganglia (e.g. *Aplysia* gill withdrawal, Kupfermann *et al.* 1974; gastropod feeding systems, reviewed by Benjamin, 1983), motoneurones innervating the muscles used during whole-body withdrawal occur in seven ganglia of the CNS. The morphology, electrotonic coupling, motor fields and effects of these cells on intra- and extracellularly recorded activity of the muscles are described. In the following paper (Ferguson and Benjamin, 1991), the inputs received by these motoneurones after tactile and photic stimulation of the skin will be described. Preliminary reports of some of these findings have appeared elsewhere (Benjamin *et al.* 1985; Ferguson and Benjamin, 1985).

Materials and methods

Specimens of *Lymnaea stagnalis* weighing 1–4 g were bought from Gerrard and Haig Ltd (East Preston, Sussex), kept in aerated Brighton tapwater at approximately 20°C and fed on lettuce.

Anatomical experiments

Experiments were performed to determine (1) the arrangement and distribution of the muscles mediating the withdrawal response and the nerves innervating these muscles, (2) the central location of putative motoneurones with projections in these nerves and (3) the morphology of these motoneurones.

Muscle arrangement and innervation

The arrangement and distribution of muscles within the head-foot were examined in animals that had been anaesthetized by immersion in a mixture of Nembutal ($1\,g\,l^{-1}$) and MS222 ($3\,g\,l^{-1}$) (Lever *et al.* 1964) and then fixed. Anaesthetization ensured that the muscles remained in the relaxed state, when their orientation was more obvious. Fixation with Stieve's fixative made muscle fibres whiter and thus easier to see (Plesch *et al.* 1975). The nerves innervating the body wall muscles of *Lymnaea* were identified by dissecting their pathways from the CNS to their target organs in unfixed material.

Identification of putative motoneurones

Putative motoneurones were identified by backfilling the nerves that innervated the body wall musculature. Isolated brains were maintained in Hepes saline (see Benjamin and Winlow, 1981) and cut nerve ends passed through a silicone seal into a 250 mmol l^{-1} cobaltous chloride solution. The preparation was then incubated at 10°C for 2–3 days. On completion of the backfilling procedure, the cerebral commissure was cut, and the preparation was pinned out flat and processed as described by Benjamin *et al.* (1979). Preparations were viewed in whole mount through a Leitz Orthoplan compound microscope, photographed with Kodak technical pan F black and white film (50 ASA) and drawn using a Leitz drawing tube attached to the microscope.

Motoneurone morphology

The morphology of motoneurones was revealed by intracellular ionophoresis of Lucifer Yellow CH (Stewart, 1978). Neurones were impaled with electrodes (resistance 100–200 MΩ) containing a 3% aqueous solution of Lucifer Yellow. Dye was injected into cells by passing hyperpolarizing 1 s square-wave current pulses of 5–10 nA at a frequency of 0.5 Hz for 1–3 h. The amount of current injected was monitored using an I/V converter placed between the indifferent electrode and ground. The spread of Lucifer Yellow through the soma was monitored by illumination with light passed through a blue filter. After ionophoretic injection the brain was fixed (Stewart, 1978), dehydrated in 100% methanol, cleared and mounted in methyl salicylate, and viewed as a whole mount under ultraviolet illumination using a Leitz Orthoplan microscope fitted with a K530 barrier filter. Preparations were photographed with Kodak Ektachrome Daylight colour film (400 ASA) or Ilford XP1 400 black and white film (400 ASA) and subsequently drawn using a Leitz drawing tube.

Neuronal and muscle recording

Simultaneous intracellular recordings were made from neurones and muscle fibres using glass microelectrodes filled with a saturated solution of K_2SO_4. The preparations were maintained in Hepes-buffered saline. Microelectrodes with a resistance of 20–30 MΩ were used to impale neurones with somata 80 μm or more in diameter, but higher-resistance electrodes (30–50 MΩ) were necessary to record from smaller neurones and muscle fibres. Voltage signals were fed into current injection amplifiers, displayed on a storage oscilloscope and permanently recorded using a pen-recorder. For accurate measurements of membrane potentials during current injection, neurones were impaled with two electrodes. To aid double penetration of small cells, the outer sheath of connective tissue was first softened by brief local application of a few crystals of proteolytic enzyme (Protease, type XIV, Sigma), after which the preparation was washed with several changes of normal saline. One microelectrode was used for current injection and the other for recording voltage. An I/V converter placed between the indifferent

electrode and ground monitored current injection. Extracellular recordings from muscle fibres were made using conventional glass suction electrodes. Signals were fed from the electrode to a storage oscilloscope *via* a.c.-coupled amplifiers. Motor fields of individual motoneurones were mapped by moving the suction electrode over the surface of the muscle and recording one-for-one extracellular junctional potentials (EJPs, but see Chiel *et al.* 1986, for a discussion of activity recorded extracellularly from gastropod muscles) evoked by suprathreshold depolarization of motoneurones.

Preparations used for electrophysiological recording

Two large muscles were involved in whole-body withdrawal, the columellar (CM) and the dorsal longitudinal (DLM) muscles (see Figs 1, 2). Together these muscles covered most of the internal surface of the body wall (Fig. 2) and different preparations were necessary to record from the muscle fibres and motoneurones of the different muscle systems (Fig. 1). Both preparations consisted of the deshelled and eviscerated head-foot. To record from the CM and its motoneurones, a longitudinal incision was made along the dorsal midline of the head-foot to expose the CM, leaving its innervation intact (Fig. 1A). For studies of the DLM and its innervation, the incision was made along the ventral midline of the foot (Fig. 1B). In both types of preparation the head-foot was pinned out flat with the internal surface of the body wall uppermost. All nerves other than those innervating the CM and DLM were cut. The CNS was then pinned, dorsal surface uppermost, on a

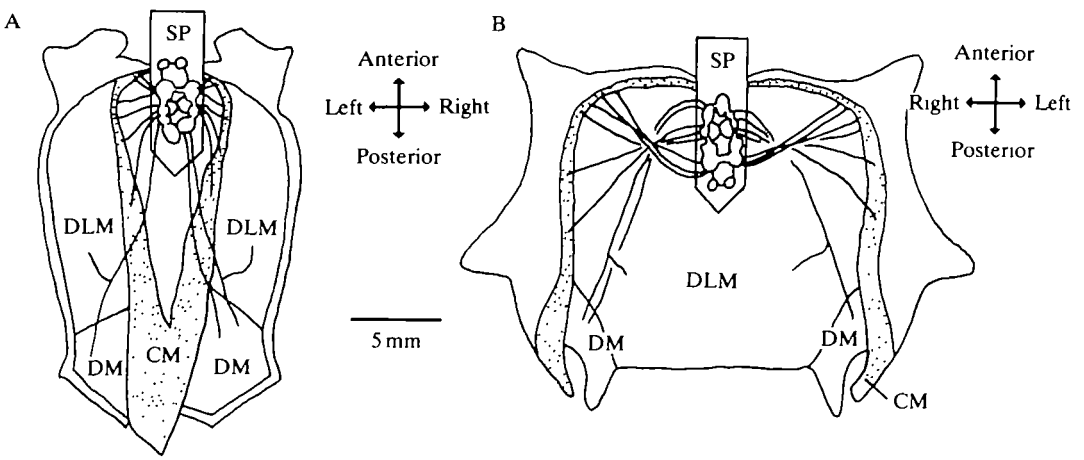

Fig. 1. Schematic illustrations of preparations used to identify motoneurones innervating the muscles used during whole-body withdrawal. For studies of the columellar muscle (CM) (A) a longitudinal cut was made along the dorsal midline of the body wall and the muscles were pinned dorsal surface uppermost. To investigate the innervation of the dorsal longitudinal muscle (DLM) (B) the cut was made along the ventral midline and muscles were pinned out ventral surface uppermost. In both preparations the brain was pinned on a platform, dorsal surface up. DM, diaphragm muscle; SP, Sylgard-covered platform.

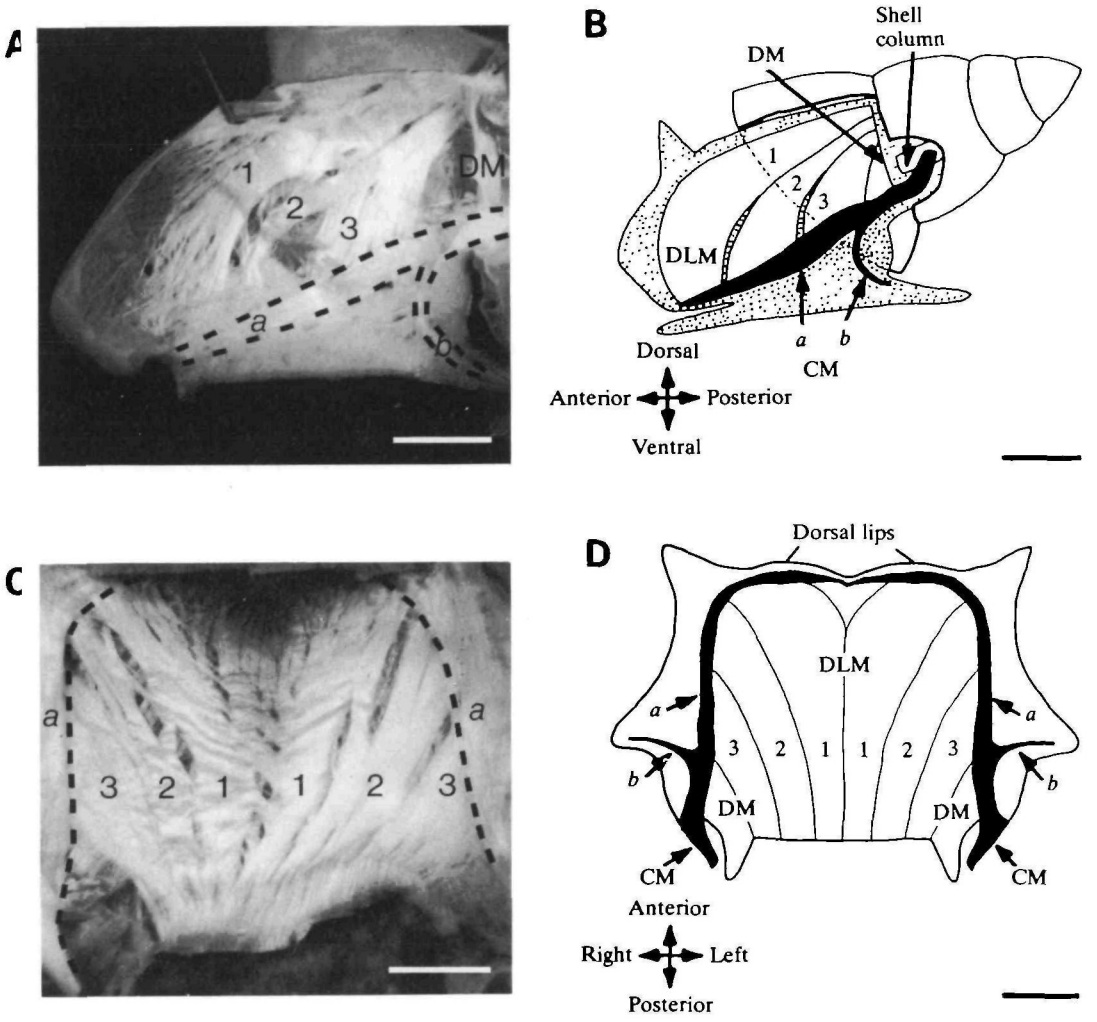

Fig. 2. Organization of the muscles mediating whole-body withdrawal. (A,B) A longitudinal hemi-section of a snail, viewed from its midline. (C,D) A ventral view of the DLM and CM. On either side of the body there were three bands of the DLM (1, 2 and 3). These had anterior origins lateral to the lateral bands on the CM (*a*) and covered the dorsal surface of the head-foot. On either side of the head-foot a lateral branch of the CM ran posteriorly from behind the dorsal lips. The lateral branches fused at the posterior end of the foot. At the point of this fusion they were joined by a band of muscle that ran up the posterior midline of the foot (*b*). The muscle then inserted onto the column of the shell. DM, diaphragm muscle. Scale bars, 5 mm.

Sylgard (Dow-Corning) covered platform suspended above the muscle part of the preparation. In DLM preparations (Fig. 1B) it was necessary to turn the CNS through 180° because the CM and DLM motoneurones were located on the dorsal surface (see Fig. 4). Once the CNS had been pinned in this position, the outer layer of connective tissue (covering its surface) was surgically removed to aid in the

penetration of the motoneurones. These CNS–muscle preparations were also used for studies of motoneurone anatomy using intracellular ionophoresis of Lucifer Yellow. Isolated brain preparations were used to examine synaptic connections between motoneurones.

Results

Organization of the muscles used during whole-body withdrawal

Whole-body withdrawal responses of *Lymnaea* can be induced by photic (light off or shadow) or strong tactile stimuli applied to the skin of the animal (Cook, 1970; Lever *et al.* 1977). Presentation of these sensory stimuli to semi-intact preparations (Fig. 1) caused the contraction of two well-developed muscle systems, the columellar muscle (CM) and the dorsal longitudinal muscle (DLM). These muscles formed layers of tissue beneath the skin and covered most of the dorsal and lateral regions of the body (Fig. 2). Muscle insertions occurred at a number of points, including the foot and the shell, and shortening contractions of the CM and DLM accounted for the main movements underlying whole-body withdrawal.

The CM, for most of its length, consisted of a pair of bilaterally symmetrical bands which ran laterally on either side of the body, internal to the DLM (labelled *a* in Fig. 2). Along their entire length, fibres from these lateral bands ran into the diffuse musculature of the foot. At the anterior end of the body, fibres from both lateral bands converged towards the midline and interdigitated with muscles from the opposite side of the body. Towards the posterior end of the head region, the lateral bands were joined by a third, ventrally inserted muscle band (*b* in Fig. 2), which ran up the posterior midline of the foot and joined the fused lateral branches to form a common root that continued posteriorly and eventually inserted onto the column of the shell (Fig. 2B). Contraction of the lateral branches of the CM shortened the ventral areas of the head-foot, whilst the more ventral, posterior CM branch shortened the posterior foot in the same anterior–posterior axis. In the intact animal the longitudinal shortening of the body was accompanied by the forward and downward pulling of the shell (*via* the CM insertion on the column of the shell) to cover the head-foot.

The rest of the head-foot was covered by a continuous layer of DLM muscle which extended over the entire dorsal surface of the animal. This consisted of two sets of three bands (labelled 1, 2 and 3 in Fig. 2) of bilaterally symmetrical muscle which lay to the left and right side of the midline of the dorsal surface of the body. The right-hand muscles are shown in lateral view (from the midline) in Fig. 2A,B and the complete set in ventral view in Fig. 2C,D. On each side of the body, band 1 ran from behind the dorsal lips at the anterior end of the head-foot and ended posteriorly beneath the origin of the mantle flap. Bands 2 and 3 also terminated beneath the origin of the mantle flap, but their anterior origin was lateral and posterior to that of band 1 and within the diffuse musculature of the foot, below the lateral branches of the CM. In Fig. 2A,C,D the shell has been removed so it is

not possible to see the position of the posterior end of the DLM in relation to it. However, by examining animals with the shell still attached, it was found that the posterior end of the DLM lay in the suture of the first whorl of the shell (Fig. 2B). When the DLM contracted, the dorsal head-foot was shortened in the anterior–posterior axis and thus the actions of the DLM complemented those of the CM. During the shortening of the body occurring in the withdrawal response both muscles were active together (see Fig. 2 of Ferguson and Benjamin, 1991).

Neural innervation of the CM and DLM

The nerve supply to the CM was restricted to the paired columellar nerves that originate from the lateral edge of the pedal ganglia (see Fig. 4) and project ipsilaterally to the lateral bands of the CM. The work of Cook (1975) suggested that the CM was also innervated by the inferior and superior cervical nerves. In the present study these nerves were found to pass through the CM (to the DLM) without providing an innervation. The innervation of the DLM was more complex than that of the CM, involving three pairs of nerves. The main innervation came from the inferior and superior cervical nerves, which arise from the lateral edge of the pedal ganglia (see Fig. 4), close to the pedal-pleural and cerebro-pedal connectives, and project to the DLM. The superior cervical nerves innervated the anterior part of the DLM and the inferior cervical nerves innervated the posterior region (see Fig. 7). Another minor innervation came from small branches of the left and right parietal nerves, which project ipsilaterally to the central regions of the DLM.

The innervation pattern described here accounts for the results of Cook (1975), who showed that the major part of the whole-body withdrawal response was abolished by cutting the columellar and cervical nerves. A small component of the response remained and we presume that this was due to the parietal nerves remaining intact.

Identification of putative motoneurones

As a first step in the identification of motoneurones innervating the CM and DLM, the columellar and cervical nerves (the main nerves innervating the CM and DLM) were backfilled with cobaltous chloride (Pitman *et al.* 1972). Backfills of either partner of these bilaterally symmetrical pedal nerves gave similar, approximately mirror-image patterns of cell body distribution within the cerebral, pleural and pedal ganglia, but not within the asymmetrical parietal and visceral ganglia. The positions of the somata stained after backfills of the left columellar, superior cervical and inferior cervical nerves are shown schematically in Fig. 3A,D and G, respectively (where each drawing is a composite compiled from the results of 10 backfills). Although backfilling revealed many stained cells, only the position of cells that were later found to innervate the muscles used during whole-body withdrawal will be described.

Backfills of the columellar nerve revealed two cells that were motoneurones to the CM. In the cerebral ganglion a single cell within the A cluster neurones was

stained. The soma of this cell (see Fig. 4) was on the medial edge of the A cluster (Fig. 3B) and the axon ran to the columellar nerve through the cerebro-pleural and pleuro-pedal connectives. The second cell had its soma in the G cluster (Slade *et al.* 1981) of the pedal ganglion, adjacent to the dorsal edge of the statocyst (Fig. 3C).

Backfills of the left superior and inferior cervical nerves also stained cells in the ipsilateral cerebral A cluster (Fig. 3E and H). Electrophysiological recordings later showed these cells to be motoneurones to the DLM. Typically, 9–12 cells with somata 30–60 μm in diameter were stained after backfills of either nerve. The axons of these cells followed the same pathway to the pedal ganglion as that of the cell stained in columellar nerve backfills. Backfills of both cervical nerves also stained 3–10 somata in the pedal N cluster (Slade *et al.* 1981), a cluster that contained DLM motoneurones. These cells ranged from 20 to 45 μm in diameter. An example of pedal N cells stained from a superior cervical nerve backfill is given in Fig. 3F. In addition to the cells stained in the cerebral and pedal ganglia, a single DLM motoneurone was also stained on the dorsal surface of the pleural ganglion after backfills of the inferior cervical nerve (Fig. 3I). This cell was close to the pleural D group neurones (Haydon and Winlow, 1982), but, on the basis of electrophysiological characteristics, was not a D group neurone as it did not show spikes of varying amplitude.

The cerebral A cluster

One of the most interesting results from cobalt backfilling experiments was that backfills of all three pedal nerves revealed cells with somata in the cerebral A cluster. These were a clearly identifiable group of cells very amenable to intracellular recording techniques. Fig. 4 shows the position of the A clusters as well as cells in other ganglia that were electrotonically coupled to the cerebral A cluster cells, and most of which were shown (by electrophysiological recording) to be motoneurones to the muscles used during whole-body withdrawal (see Figs 7–11). The paired, bilaterally symmetrical A clusters lay on the medial-dorsal surface of each cerebral ganglion, slightly anterior to the cerebro-pleural connective (Fig. 4). *In vivo* the 30–35 yellow-orange cells in this cluster were distinguishable from the white-orange neurosecretory neurones found in the same area of the ganglion (Benjamin *et al.* 1980). The cluster could be divided into an anterior area containing 13–17 somata with diameters of 30–40 μm and a posterior area of 14–17 somata with diameters between 30 and 80 μm. Electrophysiological experiments showed that most of the cells in the posterior region were motoneurones to the DLM (see Fig. 7). On the extreme medial edge of the cluster (midway between the cerebro-pedal and the cerebro-pleural connectives) a cell was found that was a motoneurone to the CM (see Fig. 11A). The anterior cerebral A cluster cells had similar electrophysiological characteristics to the posterior cells, but projected into the ipsi- and contralateral lip nerves, rather than the nerves innervating the CM and DLM (Ferguson, 1985). Their function is unknown.

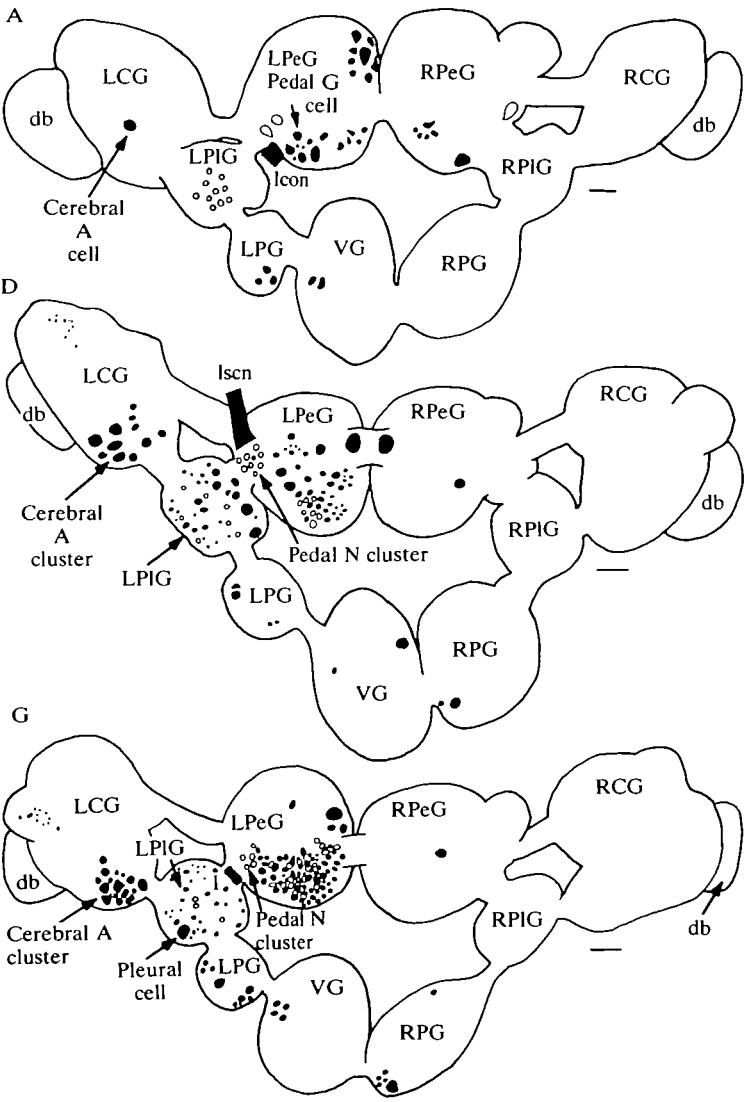

Fig. 3. Identification of putative CM and DLM motoneurones. A, D and G show, respectively, the positions of cells stained by cobalt backfilling of the left columellar, superior cervical and inferior cervical nerves (dorsally located cells shaded, ventral cells unshaded). Cells that were motoneurones are shown in the photomicrographs. Backfills of the left columellar nerve stained a single cell in the A cluster of the left cerebral ganglion (B) and the G cluster of the left pedal ganglion (C) that were CM motoneurones. Backfills of the left superior and inferior cervical nerves stained cells in the left cerebral A cluster (E and H, respectively) that were DLM motoneurones. Pedal N cluster cells (on the ventro-lateral surface of the pedal ganglia) were also stained after backfills of the superior and inferior cervical nerves; this is shown for the superior cervical nerve in F. This cluster contained DLM motoneurones. Backfills of the inferior cervical nerve stained a single cell in the left pleural ganglion that was a

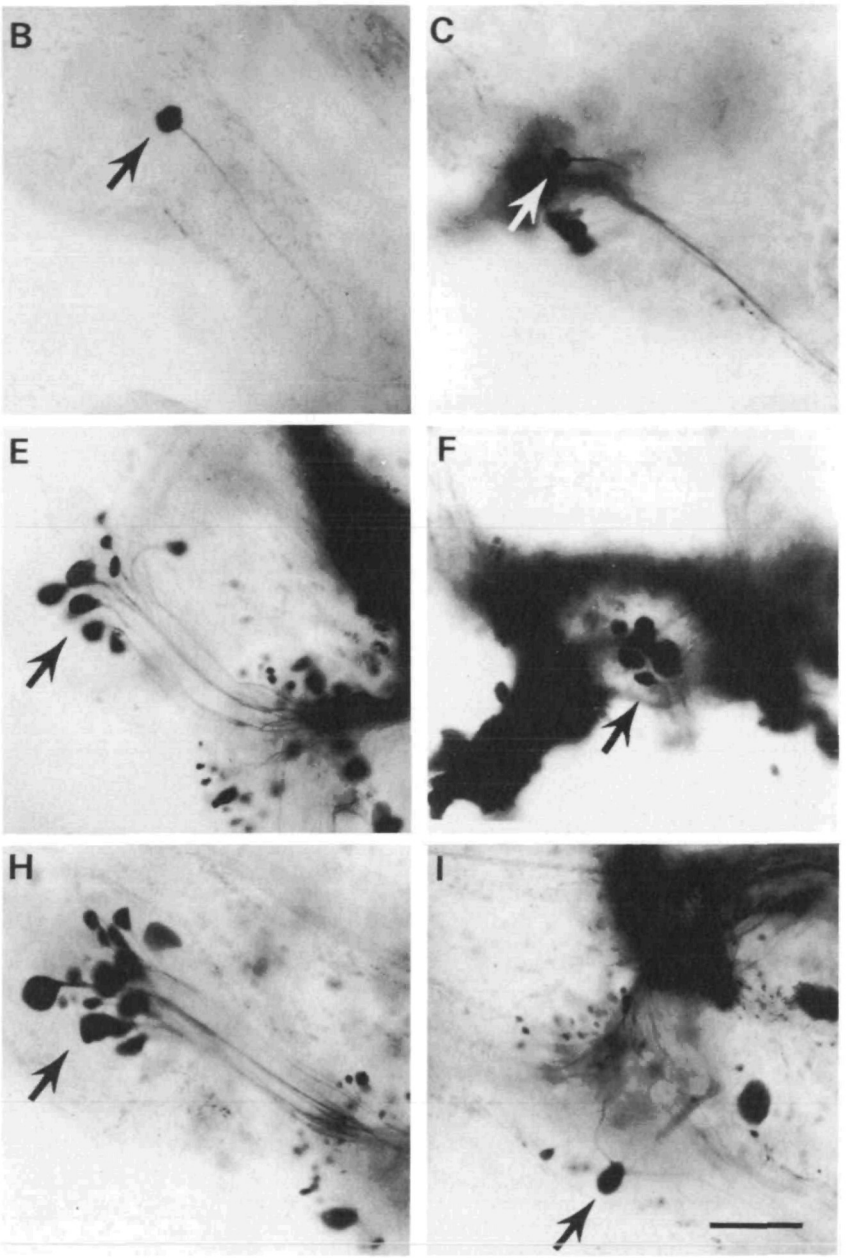

DLM motoneurone (I). Preparations were viewed dorsally after cutting the cerebral commissure and pinning the cerebral ganglia apart. LCG, RCG, left and right cerebral ganglia; LPlG, RPlG, left and right pleural ganglia; LPeG, RPeG, left and right pedal ganglia; LPG, RPG, left and right parietal ganglia; VG, visceral ganglion; lcon, left columellar nerve; lscn, left superior cervical nerve; l, left inferior cervical nerve; db, medial dorsal body. Scale bars, 125 μm.

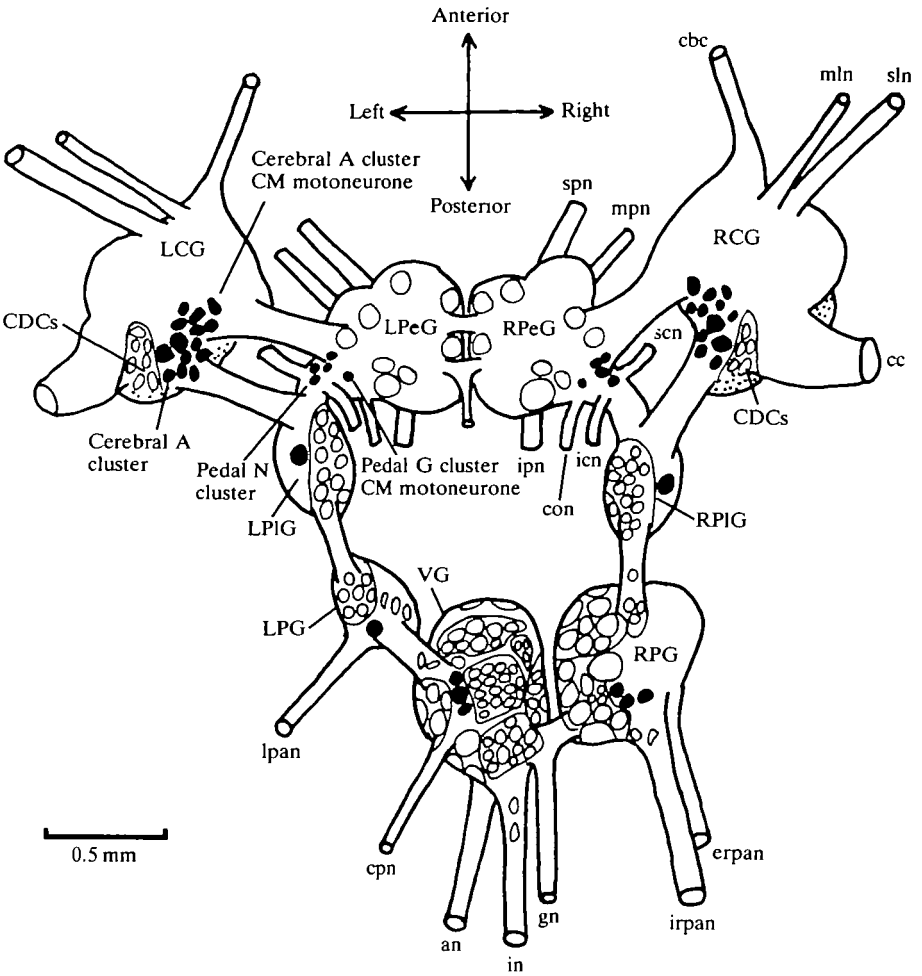

Fig. 4. Diagram showing the central positions of the electrotonically coupled cells (shaded) in relation to previously identified clusters of neurones (see Benjamin and Winlow, 1981; Benjamin *et al.* 1985; Slade *et al.* 1981). The cerebral A cluster, which contained the major group of DLM motoneurones, lies medial to the caudodorsal cells (CDCs) at the anterior end of the cerebropleural connective. On the medial edge of this cluster there was a single CM motoneurone. Another CM motoneurone occurred in the pedal G cluster. Additional DLM motoneurones occurred in the pedal N cluster and in the pleural and left parietal ganglia. No motoneuronal function was found for the electrotonically coupled cells in the visceral and right parietal ganglia. For clarity, the cerebral commissure is shown cut and the cerebral ganglia are pinned with their medial surfaces uppermost. Symmetrical nerves are labelled on the right side of the CNS only. LCG, RCG, left and right cerebral ganglia; LPG, RPG, left and right parietal ganglia; LPeG, RPeG, left and right pedal ganglia; LPlG, RPlG, left and right pleural ganglia; VG, visceral ganglion; CDCs, caudodorsal cells; cc, cerebral commissure; cbc, cerebrobuccal connective; an, analis nerve; con, columellar nerve; cpn, cutaneous pallialis nerve; erpan, external right parietal nerve; gn, genital nerve; in, intestinalis nerve; icn, inferior cervical nerve; ipn, inferior pedal nerve; irpan, internal right parietal nerve; lpan, left parietal nerve; mln, medial lip nerve; mpn, medial pedal nerve; scn, superior cervical nerve; sln, superior lip nerve; spn, superior pedal nerve.

Identification of motoneurones and general features of their effects on muscle activity

Cells previously localized by cobalt backfilling or electrophysiological recording were impaled with microelectrodes and their putative motoneuronal function was tested by examining their effects on the electrical activity of the appropriate muscles. Cells were considered to be motoneurones if they fulfilled the following criteria. (1) A reproducible and specific muscular movement was caused by the passage of suprathreshold depolarizing current into the cell. (2) A one-for-one correlation of neuronal action potentials and muscle excitatory junction potentials (EJPs) occurred with constant latency. (3) Intracellular ionophoresis of Lucifer Yellow demonstrated that the cell had the appropriate nerve projection.

All the motoneurones tested had a similar effect on intracellular muscle fibre activity and evoked one-for-one non-facilitating EJPs. Responses could be recorded from many different muscle fibres in the same muscle (Fig. 5). The resting potentials of fibres in both muscles were between -60 and -70 mV. The latency between the motoneurone action potential and the EJP was constant for individual muscle fibres, but varied within the range 7–12 ms for different muscle fibres innervated by the same motoneurone. The amplitudes of the EJPs recorded varied between 2 and 15 mV, and they had a duration of between 50 and 250 ms (Fig. 5A). The range of amplitudes and durations recorded was probably due to the variable position of the electrode relative to the neuromuscular junction or to electrotonic coupling between muscle fibres. In either case, EJPs would be attenuated in size and increased in duration by the effects of membrane leakage and capacitance as they spread electrotonically from the neuromuscular junction to the recording electrode. No all-or-nothing action potentials were recorded in either the DLM or the CM, either by direct application of steady depolarizing currents to the muscle fibres or by motoneurone activation. Intracellular and extracellular recordings from the same area of muscle gave equivalent results in localising responses to motoneuronal stimulation (see Fig. 6), although the large tips of the extracellular electrodes (typically 0.25–0.5 mm in diameter) must have been recording from many muscle fibres; in contrast, single fibres are recorded with intracellular recording. This suggests that a particular motoneurone innervates many adjacent muscle fibres, resulting in the synchronous compound EJPs recorded with the extracellular electrode.

Most experiments were conducted on the left side of the body, where the muscles were not obstructed by the penis. However, the more limited number of experiments conducted on the right side of the body gave similar results, and motoneurones occurring in the left cerebral, pleural and pedal ganglia had counterparts with equivalent motor fields on the right side of the body.

Innervation of the DLM

Cerebral motoneurones

The motoneuronal innervation of the DLM was complex owing to the large size

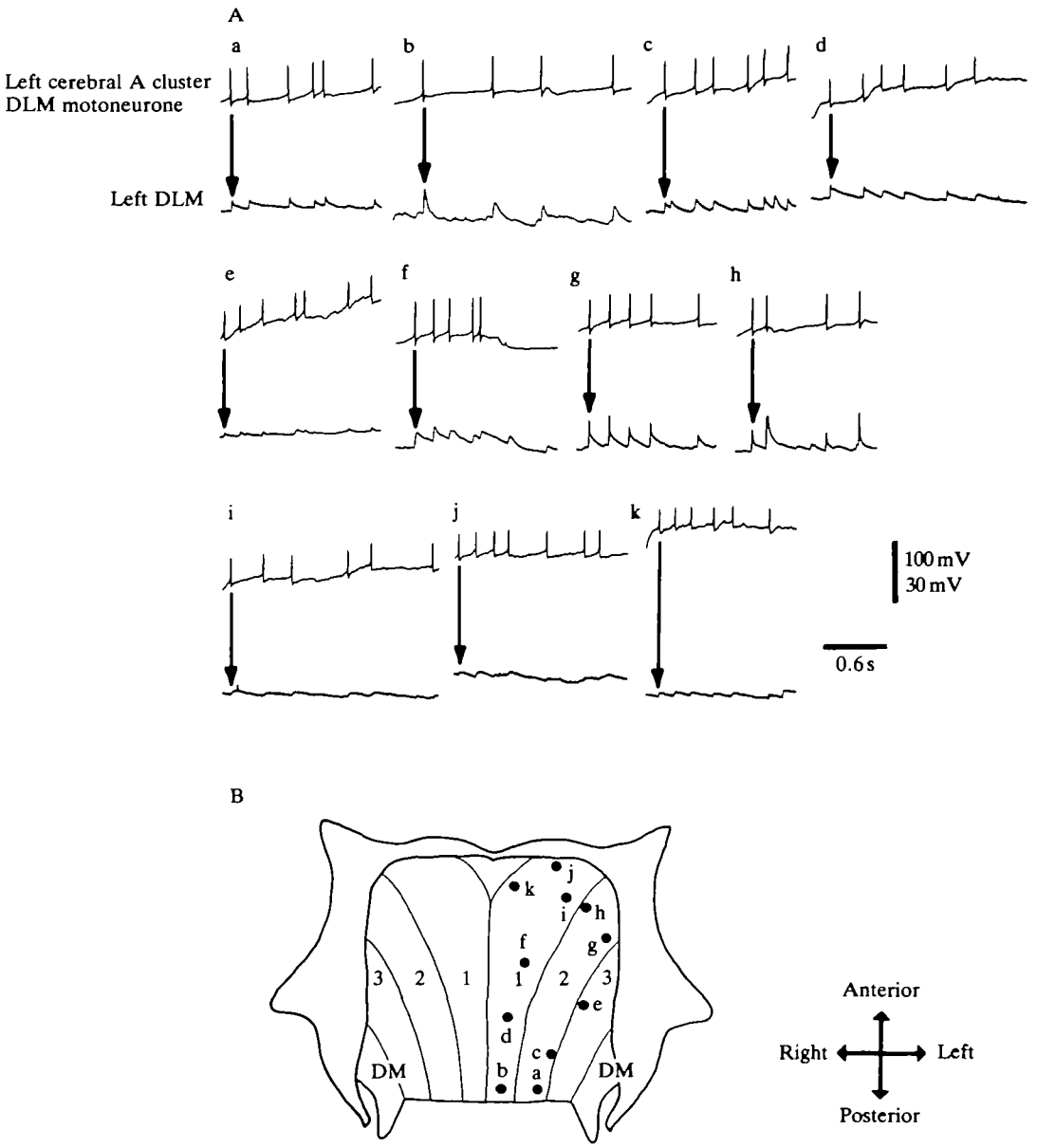

Fig. 5. General features of excitatory junctional potentials (EJPs) recorded intracellularly from the DLM. (A) Eleven recordings after depolarization of the same left cerebral A cluster DLM motoneurone. Amplitudes and durations of EJPs differed at different muscle locations (B). This is probably due to the position of the electrode relative to the neuromuscular junction or to electrotonic coupling between muscle fibres. DM, diaphragm muscle.

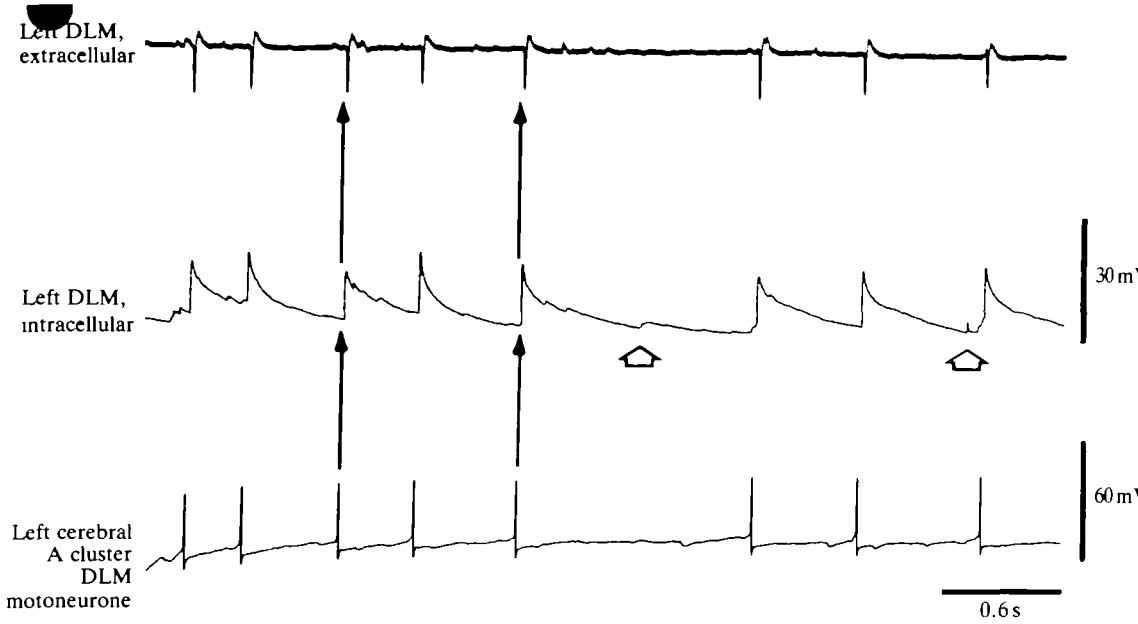

Fig. 6. Innervation of the left DLM by a left cerebral A cluster motoneurone. Action potentials in the cerebral motoneurone evoked one-for-one EJPs in the DLM. Spontaneous EJPs (open arrows) were also observed in the muscle fibre, unaccompanied by action potentials in the recorded motoneurone. These were presumably due to spikes in a second (unrecorded) motoneurone, suggesting that muscle fibres in the DLM are innervated by at least two motoneurones.

of the muscle and the presence of at least 20 motoneurones occurring in several different ganglia. The overlapping motor fields of motoneurones (e.g. Fig. 7B,D) suggested that the muscle fibres might be multiply innervated and this was supported by the occurrence of two types of EJPs in DLM muscle fibres. Low-amplitude EJPs, resulting from 'spontaneous' activity in unidentified motoneurones, were recorded with additional larger-amplitude EJPs due to evoked spikes in recorded motoneurones (Fig. 6). This suggests that at least two motoneurones innervate a particular DLM muscle fibre, although this was not directly tested by recording from two motoneurones at the same time.

Intracellular ionophoresis of Lucifer Yellow into cerebral A cluster DLM motoneurones (N=38) revealed cells with three slightly different morphologies and this correlated with the innervation pattern of the six muscle bands that form the DLM (Fig. 7). All the cells had a single axon which ran from the soma, through the cerebro-pleural connective, pleural ganglion and pleuro-pedal connective, and entered the pedal ganglion. From the pedal ganglion the axon projected into the superior cervical nerve (Fig. 7A), the superior and inferior cervical nerves (Fig. 7C) or the inferior cervical nerve (Fig. 7E). Irrespective of the peripheral projection of the motoneurone, there were usually neuritic areas within the pleural and pedal ganglia. Some cells (not shown Fig. 7) also had

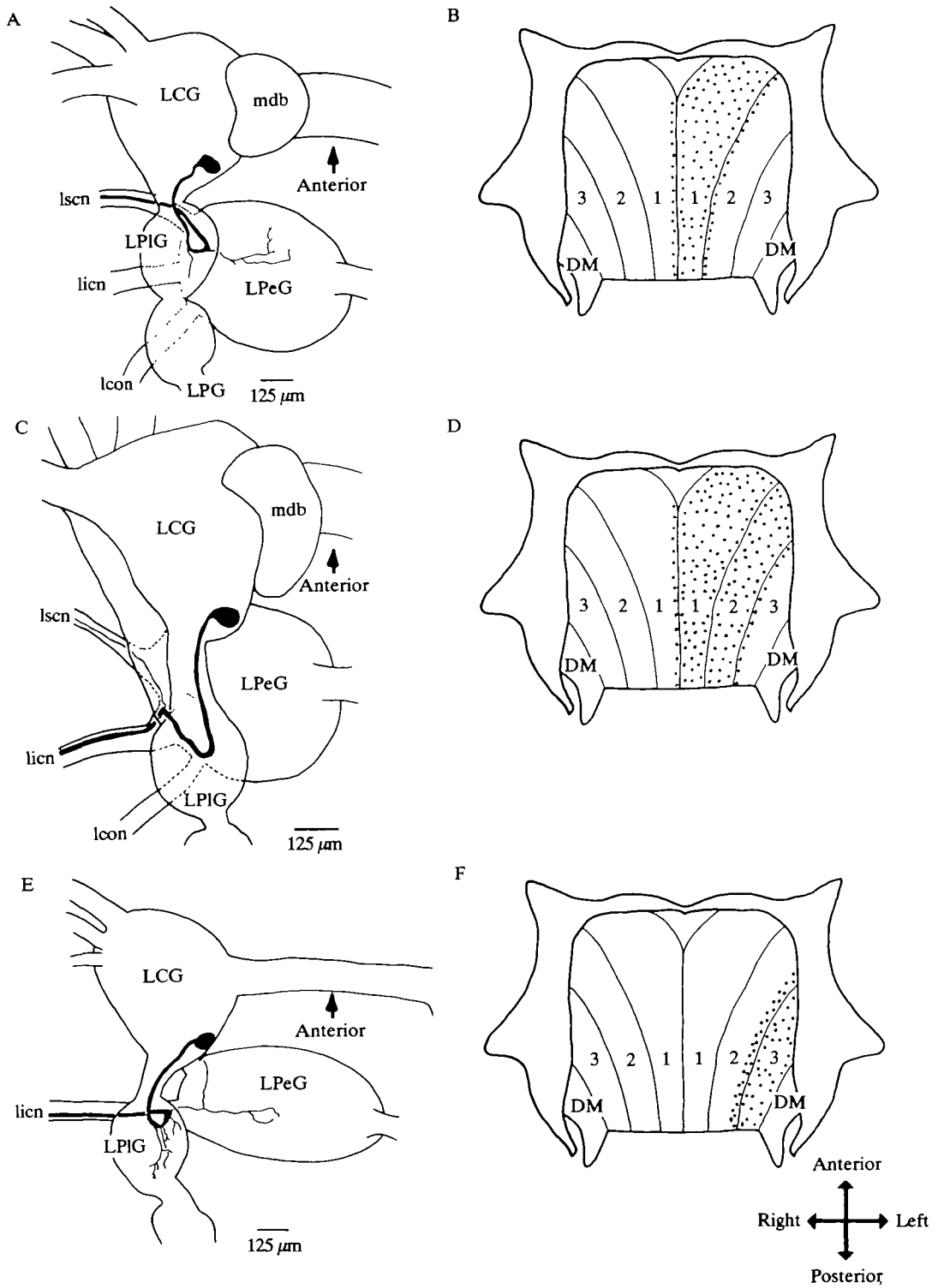
A
LCG
mdb
Anterior
lscn
LPlG
licn
LPeG
lcon
LPG
125 μm
B
3 2 1 1 2 3
DM
DM
C
LCG
mdb
Anterior
lscn
LPeG
licn
LPlG
lcon
125 μm
D
3 2 1 1 2 3
DM
DM
E
LCG
Anterior
LPeG
licn
LPlG
125 μm
F
3 2 1 1 2 3
DM
DM
Anterior
Right
Left
Posterior

Fig. 7

Fig. 7. Anatomy and motor fields of left cerebral A cluster DLM motoneurones. Cerebral motoneurones (*camera lucida* drawings) had projections into the superior cervical (A), superior and inferior cervical (C) or inferior cervical nerve (E). This difference in anatomy was reflected in the motor fields (stippled in B, D and F). LCG, left cerebral ganglion; LPG, left parietal ganglion; LPeG, left pedal ganglion; LPlG, left pleural ganglion; lcon, left columellar nerve; licn, left inferior cervical nerve; lscn, left superior cervical nerve; mdb, medial dorsal body; DM, diaphragm muscle.

neurites within the cerebral ganglion (Ferguson, 1985). In Fig. 7B,D,F the three bands of the DLM on either side of the body are shown diagrammatically and labelled 1, 2 and 3. A relationship was found between the peripheral projection of the motoneurones and the area of the DLM innervated. Motoneurones with a projection into the superior cervical nerve usually innervated the whole of band 1 (Fig. 7B), although on two occasions cells were recorded which had much more limited motor fields and only innervated the most anterior part of band 1 (not shown). Motoneurones projecting into both cervical nerves had the largest motor fields and innervated either the whole of bands 1 and 2 (Fig. 7D), or band 1 and the medial half of band 2 (not shown). Three different motor fields were found for cells with a projection into the inferior cervical nerve. The most common one included the most lateral half of band 2 and the entire band 3 (Fig. 7F). The other motor fields are not shown in Fig. 7, but were the lateral one-third of band 1 and the medial two-thirds of band 2, or all of band 2. The maximum number of motoneurones found in a single preparation was six.

It is clear from Fig. 7 that motoneurones have discrete but partially overlapping fields of innervation in the DLM. If the innervation covered several bands, then they tended to be adjacent to each other. For instance, the left cerebral A cluster cell of Fig. 7D innervated the entire ipsilateral bands 1 and 2, and had a slight overlap of innervation onto the adjacent edges of ipsilateral band 3 and contralateral band 1. The motoneurone in Fig. 7F innervated band 3 and the lateral half of band 2. Activation of the cerebral A cluster DLM motoneurones produced a longitudinal contraction of the DLM in the anterior–posterior axis, indicating that the activity of these cells could account for the shortening of the dorsal head-foot that occurs during whole-body withdrawal.

Pedal motoneurones (pedal N cells)

Not all the cells in this cluster had a motoneuronal effect on the DLM and the maximum number of motoneurones found in a single preparation was two. All the N cells that were motoneurones innervated the whole of band 3 of the muscle and the adjacent part of band 2 (Fig. 8B), produced one-for-one EJPs (Fig. 8A) and caused a longitudinal contraction. No successful fills of N cluster motoneurones with Lucifer Yellow were obtained after its motor field had been mapped. However, cobalt backfills of both cervical nerves stained cells in this cluster (see Fig. 3) and these were probably the same as those recorded in electrophysiological experiments.

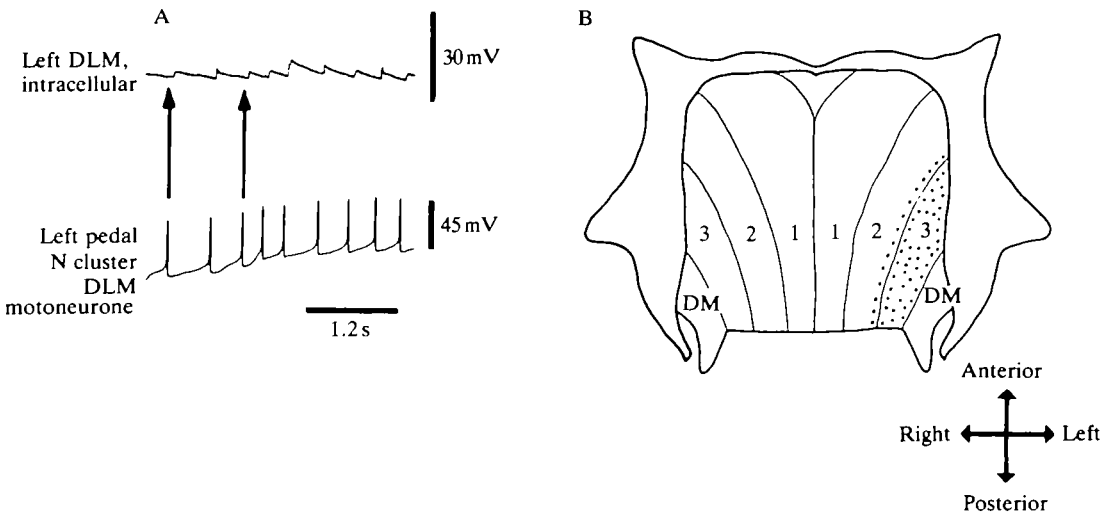

Fig. 8. Suprathreshold depolarization of a left pedal N cluster DLM motoneurone caused one-for-one EJPs (intracellular recording) in the DLM (A) and visually observed contraction of the motor field (B, stippled). DM, diaphragm muscle.

Pleural and parietal motoneurones

A single DLM motoneurone was found in the left (Fig. 9) and right pleural ganglia and the left parietal ganglion (Fig. 10). Up to three cells with similar electrical properties were found in the right parietal ganglion. These were probably DLM motoneurones but, as their effects on muscle fibres were not tested, this can only be conjectured.

Only extracellular recordings were obtained for the pleural and left parietal motoneurones (Figs 9A, 10A) but, as intracellular and extracellular recordings gave equivalent results for other motoneurones (e.g. Fig. 6), we can be reasonably sure that the motor fields in Figs 9B and 10B are correct. Each motoneurone spike produced one-for-one activity in the DLM (Figs 9A, 10A) and the DLM underwent a longitudinal contraction. The left pleural cell innervated the whole of band 2, the adjacent one-third of band 1 and the adjacent edge of band 3 (Fig. 9B). The left parietal cell had a smaller motor field and only innervated band 2 and the adjacent edges of bands 1 and 3 (Fig. 10B).

The morphology of the pleural cell (N=4 Lucifer Yellow fills) was more complicated than that of the cerebral A cluster neurones. Three axons left the cell. One of these ran posteriorly and projected into the left parietal nerve and the cutaneous pallialis nerve. A second axon ran anteriorly into the cerebral ganglion and ended there in a neuritic arborization. The third axon ran through the pleural-pedal connective and the pedal ganglion, into the inferior cervical nerve and the columellar nerve. Although this cell had projections into the inferior cervical and left parietal nerves, it is not known which of the axonal branches entering these nerves innervated the DLM. The left parietal motoneurone (N=5 Lucifer Yello

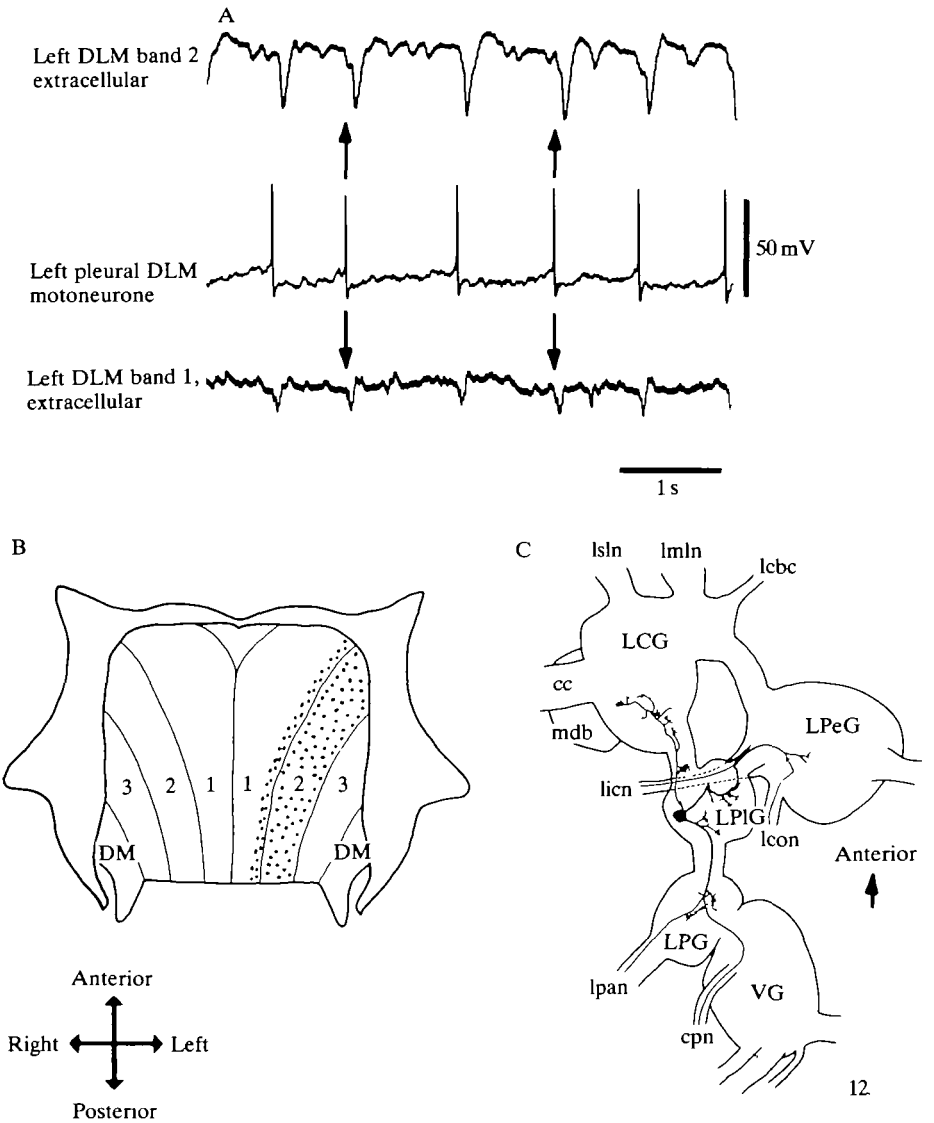

Fig. 9. Characterization of the left pleural ganglion DLM motoneurone. Suprathreshold depolarization of the motoneurone (A) elicited one-for-one EJPs (extracellular recording) in the ipsilateral DLM (motor field stippled in B). The neurone had projections to the cerebral ganglion and into the left inferior cervical, columellar, parietal and cutaneous pallialis nerves (C, *camera lucida* drawing). LCG, left cerebral ganglion; LPG, left parietal ganglion; LPeG, left pedal ganglion; LPlG, left pleural ganglion; VG, visceral ganglion; cc, cerebral commissure; cpn, cutaneous pallialis nerve; lcbc, left cerebrobuccal connective; lcon, left columellar nerve; licn, left inferior cervical nerve; lmln, left medial lip nerve; lpan, left parietal nerve; lsln, left superior lip nerve; mdb, medial dorsal body; DM, diaphragm muscle.

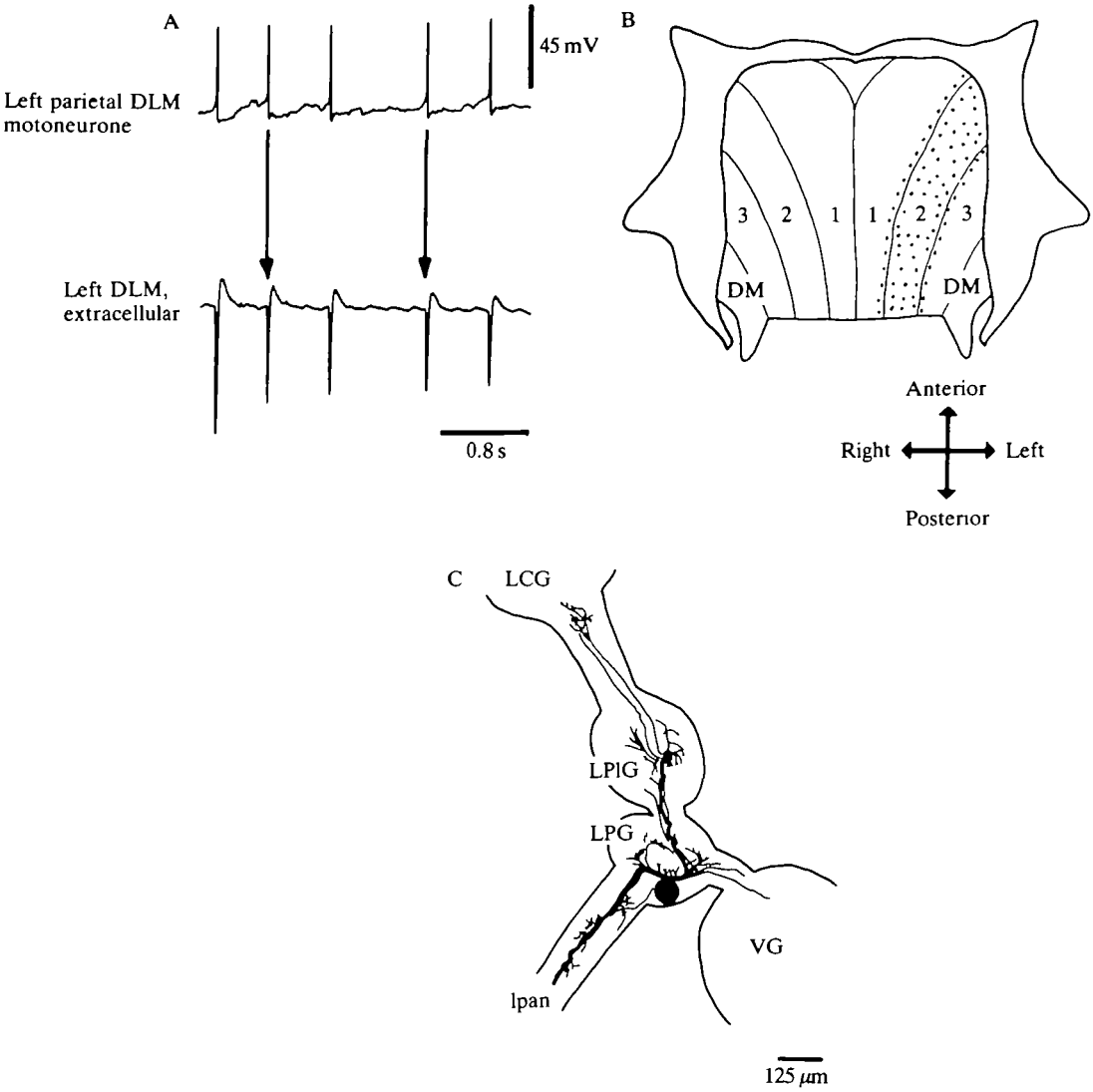

Fig. 10. Characterization of the left parietal ganglion DLM motoneurone. Suprathreshold depolarization of the motoneurone (A) produced one-for-one activity (extracellular recording) in the DLM (motor field stippled in B). The cell had a major central projection to the left pleural and cerebral ganglia and a peripheral projection into the left parietal nerve. LCG, left cerebral ganglion; LPG, left parietal ganglion; LPlG, left pleural ganglion; lpan, left parietal nerve; DM, diaphragm muscle.

injections) had a large soma (about 90 μm in diameter) located at the posterior end of the left parietal ganglion (Fig. 10C). The major axon (approximately 18 μm in diameter) projected to the DLM *via* the left parietal nerve. A second axon ran anteriorly and ended in neuritic arborizations in the pleural and cerebral ganglia. Some fine fibres left this second axon and ran posteriorly into the visceral ganglion

In summary, we can say that at least 10 motoneurones, in four separate ganglia, innervated each side of the DLM. The innervation areas of the left pleural and parietal ganglia overlapped to some extent with those of the cerebral A cluster cells. The pedal N cluster DLM motoneurone innervation areas also overlapped with those of some cerebral A cluster cells, but were distinct from those of the left pleural and parietal ganglia. All these motoneurones produced a longitudinal contraction of the DLM, suggesting that their combined activity may mediate the shortening of the dorsal head-foot during whole-body withdrawal.

Innervation of the CM

The two CM motoneurones previously identified from cobalt backfills (the cerebral A cluster cell, Fig. 3B, and the pedal G cluster cell, Fig. 3C) had similar effects on intracellular muscle activity. Each action potential in the motoneurone produced unitary 7–10 mV EJPs in the muscle fibres of the CM (Fig. 11A,B).

Intracellular ionophoresis of Lucifer Yellow showed that both cells projected into the columellar nerve. The cerebral A cluster cell (N=5 Lucifer Yellow fills) had a single axon that projected to the nerve through the cerebro-pleural connective, pleural ganglion, pleural-pedal connective and pedal ganglion (Fig. 11C). Neurites left the main axon in the cerebral, pleural and pedal ganglia. The pedal G cluster CM motoneurone (N=3 Lucifer Yellow fills) also had a single axon (Fig. 11D) which ran into the neuropile of the pedal ganglion (where it gave off neurites) before projecting into the columellar nerve.

Both motoneurones innervated the same part of the CM (Fig. 11E,F) and had motor fields that extended from about the point where the columellar nerve entered the muscle to the posterior end of the muscle, which inserted onto the column of the shell. Activation of these motoneurones could, therefore, account for the shortening of the ventral part of the head-foot and the forward movements of the shell that occur during whole-body withdrawal. More anterior regions of the muscle must be innervated by other motoneurones (see Jansen and Ter Maat, 1985; Winlow and Haydon, 1986).

Electrotonic coupling between DLM and CM motoneurones

The withdrawal response requires synchronous co-activation of motoneurones and muscles and this appears to be partly achieved by connections between the motoneurones. Paired recordings of motoneurones in the isolated brain showed that electrotonic coupling occurred between the motoneurones in the same and different ganglia (summarized in Table 1). Although it was not possible to record all possible combinations of cells because of the numbers involved (30–40), coupling appeared to be sufficiently widespread to make it an important factor in coordinating motoneuronal activity, particularly in DLM motoneurones. We emphasise that the complex spatial distribution of the motoneurones makes it difficult to interpret cell body recordings of coupling as direct or indirect (i.e. *via* one or more intervening cells) and to interpret measurements of coupling coefficients as indicators of coupling strength. In general, the ability of one

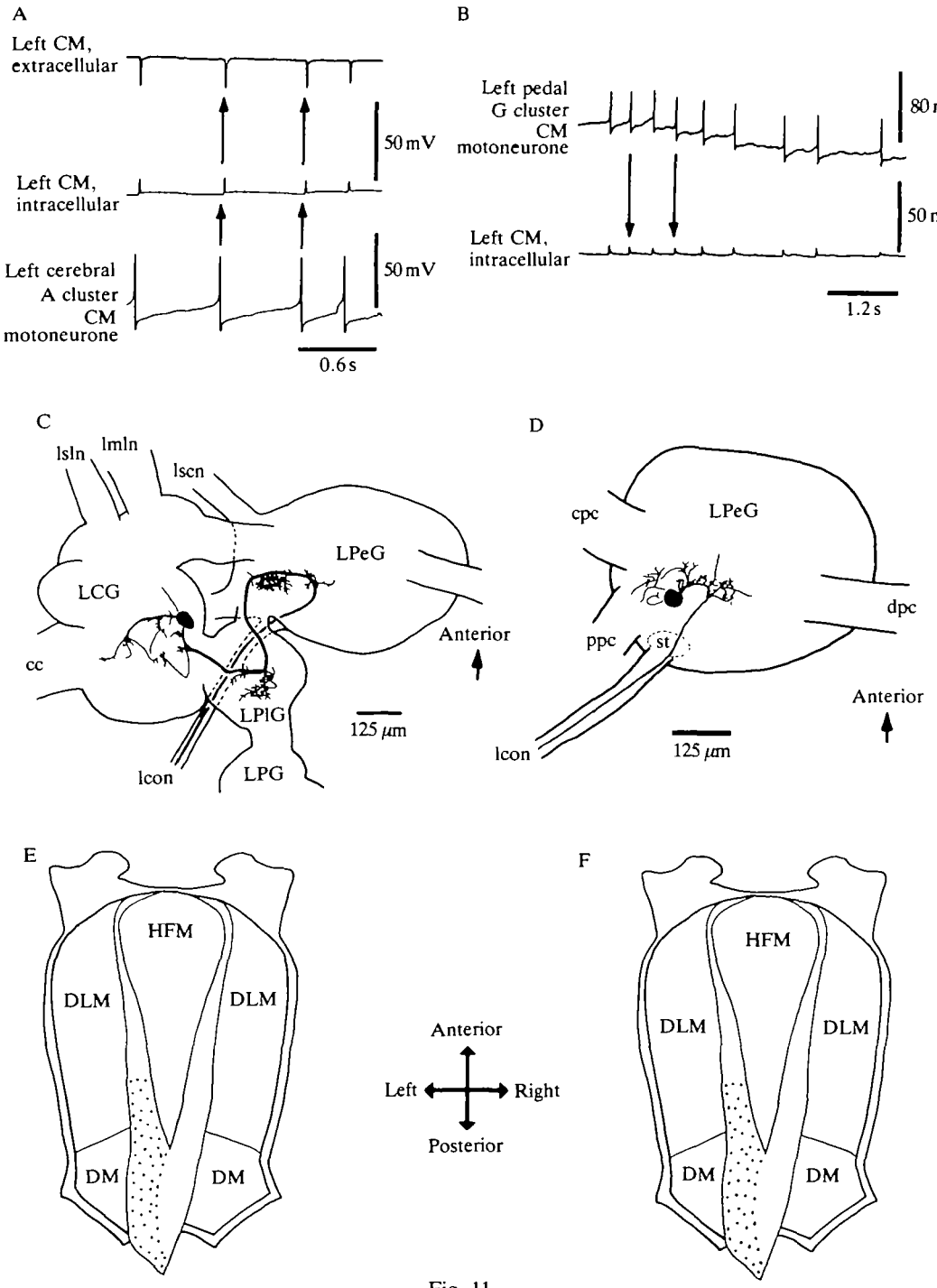
A
Left CM, extracellular
50 mV
Left CM, intracellular
Left cerebral A cluster CM motoneurone
50 mV
0.6 s
B
Left pedal G cluster CM motoneurone
80 mV
50 mV
Left CM, intracellular
1.2 s
C
lsln
lmln
lscn
LPeG
LCG
cc
Anterior
LPlG
125 μm
lcon
LPG
D
cpc
LPeG
dpc
ppc
st
Anterior
lcon
125 μm
E
HFM
DLM
DLM
DM
DM
Anterior
Left
Right
Posterior
F
HFM
DLM
DLM
DM
DM

Fig. 11

Fig. 11. Characterization of CM motoneurones. Action potentials in the left cerebral A cluster and left pedal G cluster motoneurones evoked one-for-one EJPs in the CM (A,B). Both cells projected into the columellar nerve (C,D; *camera lucida* drawings). Both cells innervated the same area of the CM (motor fields stippled in E and F). DM, diaphragm muscle; DLM, dorsal longitudinal muscle; HFM, horizontal foot muscle; LCG, left cerebral ganglion; LPG, left parietal ganglion; LPeG, left pedal ganglion; LPlG, left pleural ganglion; cc, cerebral commissure; cpc, cerebro-pedal connective; dpc, dorsal pedal commissure; lcon, left columellar nerve; lmln, left medial lip nerve; lscn, left superior cervical nerve; lsln, left superior lip nerve; ppc, pleuropedal connective; st, statocyst.

Table 1. *Pairs of electrotonically coupled neurones**

Presynaptic neurone	Postsynaptic neurone
Left cerebral A cluster DLM motoneurone	Left cerebral A cluster DLM motoneurone
Left cerebral A cluster DLM motoneurone	Left pedal N cluster DLM motoneurone
Left cerebral A cluster DLM motoneurone	Left pleural ganglion DLM motoneurone
Left cerebral A cluster DLM motoneurone	Left parietal ganglion DLM motoneurone
Left cerebral A cluster DLM motoneurone	Left pedal ganglion CM motoneurone
Left cerebral A cluster DLM motoneurone	Visceral ganglion neurone
Left cerebral A cluster DLM motoneurone	Right parietal ganglion neurone
Right cerebral A cluster DLM motoneurone	Right cerebral A cluster DLM motoneurone
Right cerebral A cluster DLM motoneurone	Right pedal N cluster DLM motoneurone
Right cerebral A cluster DLM motoneurone	Right pleural ganglion DLM motoneurone
Right cerebral A cluster DLM motoneurone	Right parietal ganglion neurone
Left parietal ganglion DLM motoneurone	Left pedal ganglion CM motoneurone
Left parietal ganglion DLM motoneurone	Visceral ganglion neurone

* It should be noted that because of the large number of electrotonically coupled neurones (see Fig. 4) it was not possible to test all possible combinations of pairs of cells.

motoneurone to induce one-for-one EPSPs and/or spikes was interpreted to indicate a strong connection and this occurred commonly in cells from the same (ipsilateral side) of the ganglionic ring.

One example of the type of experiment used to examine the coupling between motoneurones (in this case a left cerebral A cluster neurone and a left parietal neurone, both DLM motoneurones) is shown in Fig. 12. A square current pulse was injected into the left cerebral A cluster cell through one electrode and the voltage change this produced was measured through a second electrode within the same cell. A similar, but attenuated, voltage change was recorded in the left parietal cell (Fig. 12A). A range of current values was injected (typically from -10 to $+10$ nA) and positive and negative d.c. coupling coefficients (ratio of voltage change in the postsynaptic cell to that in the presynaptic cell) were calculated. The I/V relationships of pre- and postsynaptic cells were also plotted (Fig. 12B). The mean coupling ratio for this pair of cells was 0.32. The difference in the slopes for

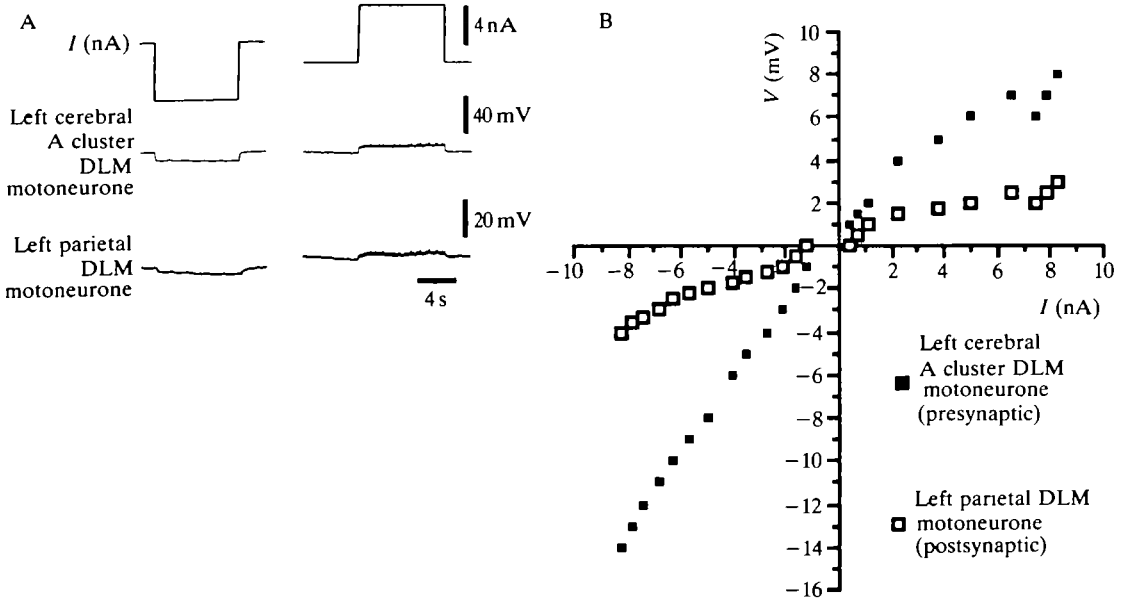

Fig. 12. Electrotonic coupling between a left cerebral A cluster DLM motoneurone and the left parietal ganglion DLM motoneurone. (A) A square current pulse injected into the cerebral cell (top trace) caused a voltage change in the presynaptic cell and a smaller voltage change in the postsynaptic cell. (B) Plotting the I/V relationship for each cell produced a slope for positive current injection that was slightly flatter than that for negative current.

positive and negative current (with the slope for positive current being slightly flatter than that for negative current) was found for all motoneurones and is typical of plots produced for other electrotonically coupled cells (e.g. Sandeman, 1971). No clear rectification was seen on the negative part of the slope, unlike that reported for the metacerebral cells of *Aplysia* (Kandel and Tauc, 1966).

The d.c. coupling coefficients between motoneurones ipsilateral to each other varied from 0.03 to 0.35 (N=24), but even for the same types of cells there were variations in the coupling coefficients (e.g. the coefficient between left cerebral A cluster neurones and the left parietal motoneurone ranged from 0.08 to 0.32, N=5). When cells on the opposite sides of the brain were recorded together the d.c. change in the postsynaptic cells was difficult to see and often only postsynaptic potentials were obvious in response to spikes. This difference in the strength of coupling between cells on the same side, and on opposite sides, of the brain is illustrated in Fig. 13, which shows the effect of depolarizing current injected into a right cerebral A cluster neurone on a right pleural neurone (Fig. 13A) and of depolarizing current injected into a left cerebral A cluster neurone on a right parietal cell (Fig. 13B). Even where cells were strongly coupled (Fig. 13A), one-for-one action potentials were not usually produced in both cells. However, there was always a clear change in the d.c. level of the postsynaptic cell and actio

potentials always induced at least one-for-one EPSPs (sometimes leading to spikes). When the cells were weakly coupled (Fig. 13B) the situation was different and there were not always one-for-one action potentials or even EPSPs. This is especially noticeable at the start of the depolarizing step where high-frequency action potentials occurred in the presynaptic cell. Later in the depolarizing pulse, action potentials and electrotonic EPSPs did become one-for-one. The most likely explanation for the failure to measure d.c. coupling potentials and one-for-one action potentials and EPSPs between weakly coupled cells would be the presence of an intermediate neurone between the presynaptic and postsynaptic cells. Thus, action potentials induced in the intermediate cell might induce EPSPs, but d.c. potentials would be attenuated to the point where they could no longer be recorded.

This hypothesis is supported by Lucifer Yellow fills. These show that strongly coupled cells had common neuritic areas (e.g. cerebral A cluster neurones and pleural cells both had neurites in the pleural and pedal ganglia, Figs 7 and 9), whereas cells that were weakly coupled did not (e.g. left cerebral A cluster cells and right parietal cells, Figs 7 and 14). However, where cells were weakly coupled there were intermediate cells that had neuritic areas in common with them, through which the current may have passed. Fig. 14 shows the morphology of visceral ganglion (N=3 Lucifer Yellow fills) and right parietal ganglion (N=3 Lucifer Yellow fills) cells. These cells were part of the electrotonically coupled network of CM and DLM motoneurones (although their motoneuronal role was not examined during the present study) and their morphologies suggest that the visceral cell could be the intermediary between the left cerebral A cluster cells and right parietal cells. For instance, visceral and left cerebral A cluster cells (Fig. 7) both have neuritic arborizations within the same area of the left pleural ganglion, while visceral and right parietal cells have common neuritic areas in the right parietal ganglion.

Discussion

Evidence for motoneuronal function

This paper describes the two main muscles (the CM and DLM) whose actions underlie the main components of the whole-body withdrawal response in *Lymnaea stagnalis*: the longitudinal shortening of the body and pulling of the shell over the dorsal body surface. The innervation pattern of these muscles was complex, as was the organization of motoneurones controlling them. Altogether there were some 24–40 motoneurones (12–20 on each side) that were electrotonically coupled and distributed in seven ganglia of the CNS (Fig. 4). Additionally there were cells in the remaining two ganglia of the CNS (the visceral and right parietal) that were part of the electrotonically coupled network of cells, but whose motoneuronal function was not investigated. CM motoneurones (N=4) occurred in the pedal and cerebral ganglia and DLM motoneurones in the cerebral, pedal, pleural and left parietal ganglia ($N \geq 19$). Evidence of motoneuronal function was of two types: (a)

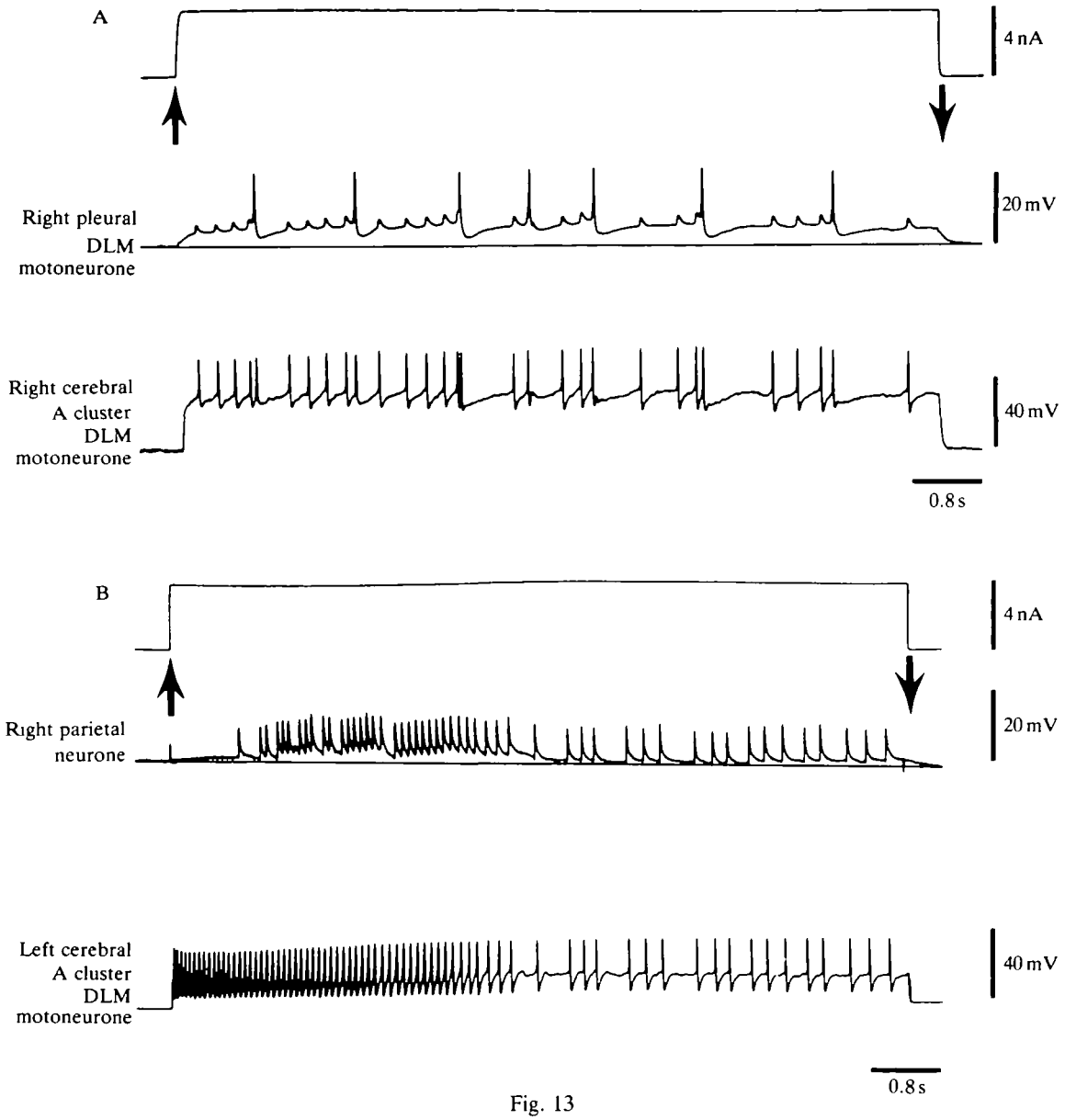

Fig. 13

simultaneous electrophysiological recording of motoneurones and muscles, demonstrating 1:1 motoneuronal spikes and muscle EJPs (intracellularly and/or extracellularly recorded) and (b) dye injection of neurones, demonstrating axonal projections along nerves known to innervate the DLM and CM. Interpretation of the electrophysiological recordings was complicated by the electrotonic coupling, which was widespread amongst motoneurones. Thus, activation of one motoneurone might be thought to co-activate other motoneurones within the motor pool. However, this is unlikely to cause the clear 1:1 recordings of motoneuron

Fig. 13. Strong and weak electrotonic coupling. Where coupling is strong (A), in this case between a right cerebral A cluster DLM motoneurone (presynaptic) and a right pleural DLM motoneurone (postsynaptic), current injection (top trace, arrows indicate current on and off) causes a d.c. change in the potential of both cells. Spikes in the presynaptic cell are followed by one-for-one EPSPs, or action potentials, in the postsynaptic cell. Where coupling is weak (B), in this case between a left cerebral A cluster DLM motoneurone (presynaptic) and a right parietal ganglion cell (postsynaptic), current injection causes a much weaker d.c. change in the potential of the postsynaptic cell. At the start of depolarization, spikes in the presynaptic cell do not cause one-for-one EPSPs in the postsynaptic cell. EPSPs start about 1 s after current injection and gradually become one-for-one in both cells, suggesting an indirect connection between them.

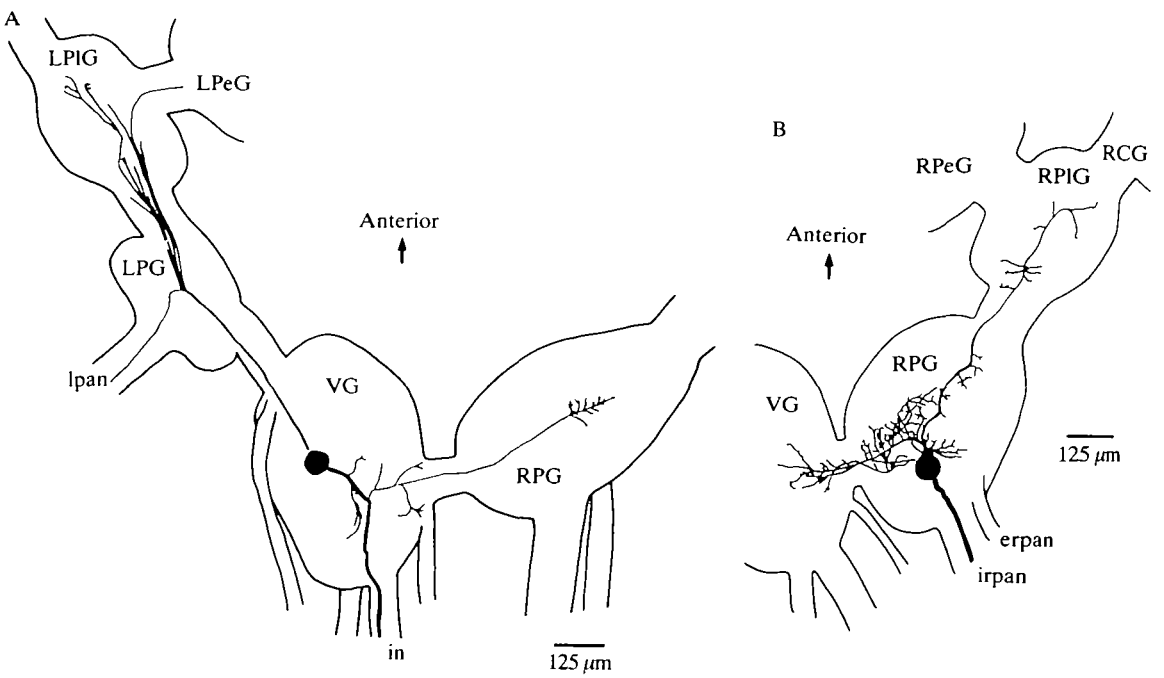

Fig. 14. Putative motoneurones in the visceral and right parietal ganglia. These cells were electrotonically coupled to the CM and DLM motoneurones (see Table 1). The visceral neurone (A) had peripheral projections into the intestinalis and left parietal nerves and central projections to the left pleural and right parietal ganglia. The right parietal cell (B) had a peripheral projection to the internal right parietal nerve and central projections to visceral and right pleural ganglia. LPG, RPG, left and right parietal ganglia; LPeG, RPeG, left and right pedal ganglia; LPlG, RPlG, left and right pleural ganglia; RCG, right cerebral ganglion; VG, visceral ganglion; erpan, external right parietal nerve; in, intestinalis nerve; irpan, internal right parietal nerve; lpan, left parietal nerve.

spikes and EJPs (Figs 5–9), especially as coupling rarely produced 1:1 firing of motoneurones in the isolated brain (Fig. 13). Similarly, coupling of the muscle fibres themselves (not investigated in the present study, but previously shown for the buccal muscles of *Aplysia californica*; Cohen *et al.* 1978; Orkand and Orkand, 1975; and *Helix pomatia*; Peters and Althrup, 1984) could also confuse the interpretation of motoneurone–muscle recordings, but here again the complex spatial configuration of muscle fibres and the rather discrete and mostly non-overlapping innervation fields of motoneurones make coupling between muscle fibres an unlikely explanation of 1:1 motoneurone spiking and EJPs.

It is of interest that one neuronal cluster, the cerebral A cluster, contained motoneurones for both the CM and DLM. This cluster of neurones was examined by Winlow and Haydon (1986) during an investigation of the neuronal control of locomotion in *Lymnaea*. They found that depolarization of cerebral A cluster neurones caused contraction of the body wall, but, unlike neurones that they identified in the pedal D and F clusters (see also, Haydon and Winlow, 1986), the cerebral A cluster neurones did not participate in spontaneously occurring locomotor behaviour. The present study extends the work of Winlow and Haydon (1986) by identifying which of the muscles of the body wall are innervated by the cerebral A cluster neurones (namely the CM and DLM). The following paper (Ferguson and Benjamin, 1991) demonstrates that at least one of the functions of the cerebral A cluster neurones is to cause contraction of the CM and DLM during whole-body withdrawal.

Innervation patterns and electrical responses of the CM and DLM

The innervation of the CM and DLM is more complicated than that of previously described gastropod motor systems. Although previous studies have shown that a particular muscle area can be innervated by neurones located within the same ganglion (Rock *et al.* 1977; Chan and Moffett, 1982) or by neurones with axons in the same nerve (Orkand and Orkand, 1975; Peters, 1979), this is the first example to show that particular areas of muscle can be innervated by motoneurones in different ganglia (e.g. the innervation of the DLM by cerebral A cluster, pedal N cluster, parietal and pleural motoneurones). The functional significance of an area of the CM or DLM being innervated by motoneurones in more than one ganglion is not clear as during whole-body withdrawal the entire CM and DLM contract together. Data presented in the following paper (Ferguson and Benjamin, 1991) show that when a particular area of the body is presented with tactile stimuli (which induce contraction in a semi-intact preparation) the sensory input causes co-excitation of many motoneurones in the network and not just of the motoneurones in one ganglion. However, it is possible that weaker tactile stimuli cause more localised withdrawal of the body owing to local sensory-motor reflexes involving the tactile fields from one particular nerve and motoneurone(s) in only one ganglion. In this case, only part of the whole network involved in whole-body withdrawal would be utilized, with some sort of gating

mechanism limiting the spread of sensory input. This would be easy to test by applying sensory stimuli of different strengths.

The major feature of intracellular recordings obtained from muscle fibres of the CM and DLM was that non-facilitating EJPs, rather than overshooting action potentials, were recorded in both the DLM and CM, either spontaneously or as a result of evoked motoneuronal spikes. These EJPs were very similar in amplitude and shape to those recorded in the penis retractor muscle of *Aplysia* (Blankenship *et al.* 1977; Rock *et al.* 1977), the pharynx muscles of *Helix* (Peters, 1979; Peters and Althrup, 1984) and the anterior aorta of *Aplysia* (Sawada *et al.* 1981), but were different from the action potentials recorded in the only previous study of gastropod body wall musculature (Kater, 1971). It should be noted that direct intracellular depolarization of *Lymnaea* muscle fibres did not produce overshooting action potentials. In contrast, Kater *et al.* (1971) found overshooting action potentials in the columellar muscle of *Helisoma*. This is the only example of overshooting action potentials to be found in gastropod muscles, although Peters and Althrup (1984) occasionally recorded non-overshooting action potentials from the pharynx muscles of *Helix*. In contrast, muscle action potentials have been recorded more frequently in other groups of molluscs, such as bivalves and cephalopods (reviewed by Peters, 1979).

No input from inhibitory motoneurones was found in the CM or DLM. Although peripheral neuromuscular inhibition has been frequently recorded in other invertebrates (Gerschenfeld, 1973), the only gastropod muscles where inhibitory junctional potentials have been recorded are the extrinsic protractor (Banks, 1975), penis retractor (Blankenship *et al.* 1977) and aorta (Sawada *et al.* 1981) muscles of *Aplysia*.

Although it was not directly proved (by simultaneous recording of two motoneurones and one muscle fibre) that muscle fibres receive multiple innervation, this is suggested by the observation that two types of EJP (one spontaneous and the other evoked) could be recorded from the same muscle fibre, and by the overlapping innervation areas of motoneurones. There is further anatomical evidence from electron microscopy (Plesch, 1977), which showed that some *Lymnaea* muscle fibres receive innervation from more than one axon ending.

Electrotonic coupling

Electrotonic coupling between motoneurones has been frequently described in gastropod molluscs (e.g. Tauc, 1959; Frazier *et al.* 1967). One example is in *Navanax inermis*, where the motoneurones controlling the rapid feeding 'strike' of the pharynx are coupled electrotonically (Levitan *et al.* 1970; Spira and Bennett, 1972). In *Lymnaea*, electrotonic coupling has also been found between feeding motoneurones (Benjamin and Rose, 1979), between the giant cells RPD2 and VD1 (Soffe and Benjamin, 1980; Benjamin and Pilkington, 1986) and between neurosecretory neurones (Van Swigchem, 1979; De Vlieger *et al.* 1980; Ter Maat *et al.* 1983; Benjamin and Rose, 1984). However, two features of the network of DLM and CM motoneurones distinguish them from previously described systems

of electrotonically coupled cells. First, the neurones of this network are distributed throughout the CNS (Fig. 4). Second, the motoneurones controlling two muscle systems (the CM and the DLM) are electrotonically coupled. We assume that this coupling plays a role in synchronising electrical activity in this widely distributed motor network. Direct evidence for this was obtained from experiments where one cell was activated by intracellular current injection and a second (usually ipsilateral) cell was shown to spike as a result. It was not clear whether all the motoneurones were directly coupled or whether cells were interspersed. Anatomically, almost all the cells (apart from pedal motoneurones) had an axon or neuritic processes in the neuropile of the ipsilateral pleural ganglion (this is especially obvious for the parietal and visceral neurones, as there are specific projections which end with a neuritic arborization in the pleural ganglion), which could be the site of coupling. However, there are other sites where many motoneurones have common routes, e.g. the neuropile of the cerebral, pedal and parietal ganglia, and for most given pairs of motoneurones there is more than one site where coupling could occur. No double fills of motoneurones in the same or different ganglia were performed to see where the processes of the neurones made anatomical contact. Dye coupling (due to Lucifer Yellow diffusing from an injected cell to other coupled cells) could have provided evidence about the site of electrotonic coupling. During the present study dye coupling only occurred twice, however, and on both occasions it was between cells in the cerebral A cluster (Ferguson, 1985). This variability of dye coupling between neurones of *Lymnaea* has also been reported previously (Audesirk *et al.* 1982).

Considering the large number of cells innervating the muscles used during whole-body withdrawal, it is likely that the faster speed of transmission at the non-rectifying electrotonic synapse will spread the distribution of sensory excitation rapidly (see Ferguson and Benjamin, 1991) from one part of the motoneuronal network to all other cells and cause the synchronous firing necessary for coordinated contraction of both the CM and DLM.

We thank Walter Stewart for the gift of Lucifer Yellow. G.P.F. was supported by an SERC studentship.

References

AUDESIRK, G., AUDESIRK, T. AND BOWSHER, P. (1982). Variability and frequent failure of Lucifer Yellow to pass between two electrically coupled neurons in *Lymnaea stagnalis*. *J. Neurobiol.* **13**, 369–375.

BANKS, F. W. (1975). Inhibitory transmission at a molluscan neuromuscular junction. *J. Neurobiol.* **6**, 429–433.

BENJAMIN, P. R. (1983). Gastropod feeding: Behavioural and neural analysis of a complex multicomponent system. In *Neural Control of Rhythmic Movements* (ed. A. Roberts and B. Roberts), pp. 159–193. Cambridge: Cambridge University Press.

BENJAMIN, P. R., ELLIOTT, C. J. H. AND FERGUSON, G. P. (1985). Neural network analysis in the snail brain. In *Model Neural Networks and Behavior* (ed. A. I. Selverston), pp. 87–108. New York: Plenum Press.

BENJAMIN, P. R. AND PILKINGTON, J. B. (1986). The electrotonic location of low-resistance

intercellular junctions between a pair of giant neurones in the snail *Lymnaea*. *J. Physiol., Lond.* **370**, 111–126.

BENJAMIN, P. R. AND ROSE, R. M. (1979). Central generation of bursting in the feeding system of *Lymnaea stagnalis*. *J. exp. Biol.* **80**, 93–118.

BENJAMIN, P. R. AND ROSE, R. M. (1984). Electrotonic coupling and afterdischarges in the Light Green Cells: a comparison with two other cerebral ganglia neurosecretory cell types in the pond snail *Lymnaea stagnalis*. *Comp. Biochem. Physiol.* **77**A, 67–74.

BENJAMIN, P. R., ROSE, R. M., SLADE, C. T. AND LACY, M. G. (1979). Morphology of identified neurons in the buccal ganglia of *Lymnaea stagnalis*. *J. exp. Biol.* **80**, 119–135.

BENJAMIN, P. R., SLADE, C. T. AND SOFFE, S. R. (1980). The morphology of neurosecretory neurones in the pond snail *Lymnaea stagnalis* by the injection of Procion Yellow and horseradish peroxidase. *Phil. Trans. R. Soc. Ser.* B **290**, 449–478.

BENJAMIN, P. R. AND WINLOW, W. (1981). The distribution of three wide-acting synaptic inputs to identified neurons in the isolated brain of *Lymnaea stagnalis* (L.). *Comp. Biochem. Physiol.* **70**A, 293–307.

BLANKENSHIP, J. E., ROCK, M. K. AND HILL, J. (1977). Physiological properties of the penis retractor muscle of *Aplysia*. *J. Neurobiol.* **8**, 549–568.

BULLOCK, T. H. (1984). Comparative neuroethology of startle, rapid escape and giant fiber-mediated responses. In *Neural Mechanisms of Startle Behavior* (ed. R. C. Eaton), pp. 1–13. New York: Plenum Press.

CHAN, C. Y. AND MOFFETT, S. (1982). Cerebral motoneurons mediating tentacle retraction in the land slug *Ariolimax columbianus*. *J. Neurobiol.* **13**, 163–172.

CHIEL, H. J., WEISS, K. R. AND KUPFERMANN, I. (1986). An identified histaminergic neuron modulates feeding motor circuitry in *Aplysia*. *J. Neurosci.* **6**, 2427–2450.

COHEN, J. L., WEISS, K. R. AND KUPFERMANN, I. (1978). Motor control of buccal muscles in *Aplysia*. *J. Neurophysiol.* **41**, 157–180.

COOK, A. (1970). Habituation in a freshwater snail (*Lymnaea stagnalis*). *Anim. Behav.* **178**, 463–474.

COOK, A. (1975). The withdrawal response of a freshwater snail (*Lymnaea stagnalis*). *J. exp. Biol.* **62**, 783–796.

DE VLIEGER, T. A., KITS, K. S., TER MAAT, A. AND LODDER, J. C. (1980). Morphology and electrophysiology of the ovulation hormone producing neuro-endocrine cells of the freshwater snail *Lymnaea stagnalis* (L.). *J. exp. Biol.* **84**, 259–271.

FERGUSON, G. P. (1985). Neurophysiological analysis of whole-body withdrawal of the pond snail *Lymnaea stagnalis* (L.). DPhil thesis, University of Sussex, Brighton, 201pp.

FERGUSON, G. P. AND BENJAMIN, P. R. (1985). Whole-body withdrawal of the pond snail *Lymnaea stagnalis*. *Soc. Neurosci. Abstr.* **11**, 513.

FERGUSON, G. P. AND BENJAMIN, P. R. (1991). The whole-body withdrawal response of *Lymnaea stagnalis*. II. Activation of central motoneurones and muscles by sensory input. *J. exp. Biol.* **158**, 97–116.

FRAZIER, W. T., KANDEL, E. R., KUPFERMANN, I., WAZIRI, R. AND COGGESHALL, R. E. (1967). Morphology and functional properties of identified neurons in the abdominal ganglion of *Aplysia californica*. *J. Neurophysiol.* **30**, 1288–1351.

GERSCHENFELD, H. M. (1973). Chemical transmission in invertebrate central nervous systems and neuromuscular junctions. *Physiol. Rev.* **53**, 1–119.

GETTING, P. A. (1983). Neural control of swimming in *Tritonia*. In *Neural Control of Rhythmic Movements* (ed. A. Roberts and B. Roberts), pp. 89–128. Cambridge: Cambridge University Press.

GETTING, P. A. AND DEKIN, M. S. (1985). *Tritonia* swimming: A model system for integration within rhythmic motor systems. In *Model Neural Networks and Behavior* (ed. A. I. Selverston), pp. 3–20. New York: Plenum Press.

HAYDON, P. G. AND WINLOW, W. (1982). Multipolar neurons of *Lymnaea stagnalis*. I. Multiple spike initiation sites and propagation failure allows neuronal compartmentalization. *J. comp. Physiol.* **147**, 503–510.

HAYDON, P. G. AND WINLOW, W. (1986). Shell movements associated with locomotion of *Lymnaea* are driven by a central pattern generator. *Comp. Biochem. Physiol.* **83**A, 23–25.

JANSEN, R. F. AND TER MAAT, A. (1985). Ring neuron control of columellar motor neurons during egg-laying behavior in the pond snail. *J. Neurobiol.* **16**, 1–14.

KANDEL, E. R. (1976). *The Cellular Basis of Behavior*. San Francisco: Freeman.

KANDEL, E. R. (1979). *Behavioral Biology of* Aplysia. San Francisco: Freeman.

KANDEL, E. R. AND TAUC, L. (1966). Anomalous rectification in the metacerebral giant cells and its consequences for synaptic transmission. *J. Physiol., Lond.* **183**, 287–304.

KANZ, J. E., EBERLY, L. B., COBBS, J. S. AND PINSKER, H. M. (1979). Neuronal correlates of siphon withdrawal in freely behaving *Aplysia*. *J. Neurophysiol.* **42**, 1538–1556.

KATER, S. B., HEYER, C. AND HEGMANN, J. P. (1971). Neuromuscular transmission in the gastropod mollusc *Helisoma trivolvis*: Identification of motoneurons. *Z. vergl. Physiol.* **74**, 127–139.

KUPFERMANN, I., CAREW, T. J. AND KANDEL, E. R. (1974). Local reflex and central commands controlling gill and siphon movements in *Aplysia*. *J. Neurophysiol.* **37**, 996–1019.

KUPFERMANN, I. AND KANDEL, E. R. (1969). Neuronal controls of a behavioral response mediated by the abdominal ganglion of *Aplysia*. *Science* **164**, 847–850.

LEVER, A. J., DE VLIEGER, T. A. AND KRAAL, H. (1977). A behavioural and electrophysiological study of the withdrawal reaction of the pond snail *Lymnaea stagnalis* (L.) with particular reference to tentacle contraction. *P. Kon. Ned.* **C80**, 105–113.

LEVER, J., JAGER, J. C. AND WESTERVELD, A. (1964). A new anaesthetisation technique for fresh water snails, tested on *Lymnaea stagnalis*. *Malacologia* **1**, 331–338.

LEVITAN, H., TAUC, L. AND SECUNDO, J. P. (1970). Electrical transmission among neurons in the buccal ganglion of a mollusc, *Navanax inermis*. *J. gen. Physiol.* **55**, 484–496.

ORKAND, P. M. AND ORKAND, R. K. (1975). Neuromuscular junctions in the buccal mass of *Aplysia*: fine structure and electrophysiology of excitatory transmission. *J. Neurobiol.* **6**, 531–548.

PERETZ, B., JACKLET, J. W. AND LUKOWIAK, K. (1976). Habituation of reflexes in *Aplysia*: contribution of peripheral and central nervous systems. *Science* **191**, 396–399.

PETERS, M. (1979). Motor innervation of the pharynx levator muscle of the snail, *Helix pomatia*: physiological and histological properties. *J. Neurobiol.* **10**, 137–152.

PETERS, M. AND ALTHRUP, U. (1984). Motor organization in pharynx of *Helix pomatia*. *J. Neurophysiol.* **52**, 389–409.

PINSKER, H. M., KUPFERMANN, I., CASTELLUCCI, V. AND KANDEL, E. R. (1970). Habituation and dishabituation of the gill-withdrawal reflex in *Aplysia*. *Science* **167**, 1740–1742.

PITMAN, R. M., TWEEDLE, C. D. AND COHEN, M. J. (1972). Branching of central neurones: intracellular cobalt injections for light and electron microscopy. *Science* **176**, 412–414.

PLESCH, B. E. C. (1977). An ultrastructural study of the innervation of the musculature of the pond snail *Lymnaea stagnalis* (L.) with reference to peripheral neurosecretion. *Cell Tissue Res.* **183**, 353–369.

PLESCH, B. E. C., JANSE, C. AND BOER, H. H. (1975). Gross morphology and histology of the musculature of the freshwater pulmonate *Lymnaea stagnalis* (L.). *Neth. J. Zool.* **25**, 332–352.

ROCK, M. K., BLANKENSHIP, J. E. AND LEBEDA, F. J. (1977). Penis-retractor muscle of *Aplysia*: excitatory motoneurons. *J. Neurobiol.* **8**, 569–579.

SANDEMAN, D. C. (1971). The excitation and electrical coupling of four identified motoneurones in the brain of the Australian mud crab, *Scylla serrata*. *Z. vergl. Physiol.* **72**, 111–130.

SAWADA, M., BLANKENSHIP, J. E. AND MCADOO, D. J. (1981). Neural control of a molluscan blood vessel, anterior aorta of *Aplysia*. *J. Neurophysiol.* **46**, 967–986.

SLADE, C. T., MILLS, J. AND WINLOW, W. (1981). The neuronal organisation of the paired pedal ganglia of *Lymnaea stagnalis*. *Comp. Biochem. Physiol.* **69A**, 789–803.

SOFFE, S. R. AND BENJAMIN, P. R. (1980). Morphology of two electrotonically coupled giant neurosecretory neurons in the snail, *Lymnaea stagnalis*. *Comp. Biochem. Physiol.* **67A**, 35–46.

SPIRA, M. E. AND BENNETT, M. V. L. (1972). Synaptic control of electrotonic coupling between neurons. *Brain Res.* **37**, 294–300.

STEWART, W. W. (1978). Functional connections between cells revealed by dye coupling with a highly fluorescent naphthalimide tracer. *Cell* **14**, 741–759.

TAUC, L. (1959). Interaction non synaptique entre deux neurons adjacents du ganglion abdominal de *l'Aplysie*. *C. R. Hebd. Séanc. Acad. Sci. Paris* **248**, 1857–1859.

TER MAAT, A., ROUBOS, E. W., LODDER, J. C. AND BUMA, P. (1983). Integration of biphasic synaptic input by electrotonically coupled neuroendocrine Caudodorsal Cells in the pond snail *Lymnaea stagnalis*. *J. Neurophysiol.* **49**, 1392–1409.

VAN SWIGCHEM, H. (1979). On the endogenous bursting properties of 'Light Yellow' neurosecretory neurones in the freshwater snail *Lymnaea stagnalis*. *J. exp. Biol.* **80**, 55–67.

WILLOWS, A. O. D. (1967). Behavioural acts elicited by stimulation of single identifiable brains cells. *Science* **157**, 570–574.

WILLOWS, A. O. D., DORSETT, D. A. AND HOYLE, G. (1973). The neuronal basis of behavior in *Tritonia*. III. Neuronal mechanisms of a fixed action pattern. *J. Neurobiol.* **4**, 255–285.

WINLOW, W. AND HAYDON, P. G. (1986). A behavioural and neuronal analysis of the locomotory system of *Lymnaea stagnalis*. *Comp. Biochem. Physiol.* **83A**, 13–21.